

AD-787 700

AN EXPERIMENTAL INVESTIGATION OF OPEN
CAVITY PRESSURE OSCILLATIONS

Dennis L. Carr

Air Force Institute of Technology
Wright-Patterson Air Force Base, Ohio

September 1974

DISTRIBUTED BY:

NTIS

National Technical Information Service
U. S. DEPARTMENT OF COMMERCE
5285 Port Royal Road, Springfield Va. 22151

Unclassified

SECURITY CLASSIFICATION OF THIS PAGE (When Data Entered)

REPORT DOCUMENTATION PAGE		READ INSTRUCTIONS BEFORE COMPLETING FORM	
1. REPORT NUMBER GAE/AE/74S-1	2. GOVT ACCESSION NO.	3. RECIPIENT'S CATALOG NUMBER AD-787 700	
4. TITLE (and Subtitle) AN EXPERIMENTAL INVESTIGATION OF OPEN CAVITY PRESSURE OSCILLATIONS		5. TYPE OF REPORT & PERIOD COVERED AFIT Thesis	
7. AUTHOR(s) Dennis L. Carr Captain USAF		6. PERFORMING ORG. REPORT NUMBER	
9. PERFORMING ORGANIZATION NAME AND ADDRESS Air Force Institute of Technology (AU) Wright-Patterson AFB, Ohio 45433		8. CONTRACT OR GRANT NUMBER(s)	
11. CONTROLLING OFFICE NAME AND ADDRESS		10. PROGRAM ELEMENT, PROJECT, TASK AREA & WORK UNIT NUMBERS	
14. MONITORING AGENCY NAME & ADDRESS (if different from Controlling Office) Air Force Flight Dynamics Laboratory (FYA) Wright-Patterson AFB, Ohio 45433		12. REPORT DATE September 1974	
		13. NUMBER OF PAGES 74	
		15. SECURITY CLASS. (of this report) Unclassified	
		15a. DECLASSIFICATION/DOWNGRADING SCHEDULE	
16. DISTRIBUTION STATEMENT (of this Report) Approved for public release; distribution unlimited.			
17. DISTRIBUTION STATEMENT (of the abstract entered in Block 20, if different from Report)			
18. SUPPLEMENTARY NOTES Approved for public release; IAW AFR/190-17 Jerry C. Hix, Captain, USAF Director of Information			
19. KEY WORDS (Continue on reverse side if necessary and identify by block number) Cavity Oscillations Cavity Flow Shear Layer Water Table			
20. ABSTRACT (Continue on reverse side if necessary and identify by block number) An experimental study was undertaken to investigate the use of a water table to define the parameters that influence the pressure oscillations resulting from air flow over open cavities. Tests were also conducted to investigate means to eliminate or reduce these oscillations.			

DD FORM 1473
1 JAN 73

EDITION OF 1 NOV 65 IS OBSOLETE
Reproduced by
NATIONAL TECHNICAL
INFORMATION SERVICE
U. S. Department of Commerce
Springfield VA 22151

Unclassified
SECURITY CLASSIFICATION OF THIS PAGE (When Data Entered)

43
Unclassified

SECURITY CLASSIFICATION OF THIS PAGE(When Data Entered)

High-speed motion pictures of the flow over cavities on the water table provided a record of the sequence of events which occurred during a typical oscillation cycle. A comparison of these events with events derived from air studies showed that the water table can be used to predict the response of cavities to air flow over them.

The water table tests clearly showed that the transverse oscillations of the shear layer are related to the cavity oscillations. Various cavity geometries were tested on the water table for Froude numbers from 0.6 to 3.3 in an attempt to find those configurations which reduce oscillations.

The configurations which showed the greatest reduction in oscillations on the water table were investigated in a supersonic free air jet. Dynamic pressure recordings and schlieren photographs were obtained for these tests. A narrow band analysis of the pressure recordings was conducted and a plot of amplitude vs. frequency was made. A comparison of these plots with corresponding schlieren photographs again showed that a cavity with a nonoscillating shear layer produced no discrete pressure oscillations within it.

1 a

Unclassified

SECURITY CLASSIFICATION OF THIS PAGE(When Data Entered)

AN EXPERIMENTAL INVESTIGATION OF
OPEN CAVITY PRESSURE OSCILLATIONS

THESIS

Presented to the Faculty of the School of Engineering
of the Air Force Institute of Technology
Air University
in Partial Fulfillment of the
Requirements for the Degree of
Master of Science

by

Dennis L. Carr, B.S.

Captain USAF

Graduate Aerospace-Mechanical Engineering

September 1974

Approved for public release; distribution unlimited.

16

Preface

The flow over an open rectangular cavity causes a strong interaction between the free stream and the fluid within the cavity. This interaction produces pressure oscillations within the cavity. If the pressure oscillations are strong enough, they can generate structural vibrations which are harmful to the body containing the cavity. The aim of this study is to investigate pressure oscillations within open cavities and to provide possible means to reduce the oscillations.

I would like to express my sincere appreciation to Mr. D. L. Smith of the Aero Acoustics Branch, Flight Dynamics Laboratory (AFFDL/FYA), whose encouragement and suggestions helped substantially toward the completion of this report. I would also like to express my appreciation to my advisor, Dr. M. E. Franke, whose guidance aided greatly during this study.

I wish to thank Mr. C. C. Alexander from Tech Photo (4950/ENPI) for his assistance in taking motion pictures of the water table experiments. Also I wish to thank Mr. J. T. Flahive for his assistance in the laboratory and Mr. M. W. Wolfe for the work done by the AFIT shop in constructing the test sections.

Dennis L. Carr

Contents

Preface	ii
List of Figures	v
List of Tables	viii
List of Symbols	ix
Abstract	x
I. Introduction	1
Background	1
Objective	2
Scope	2
II. Discussion of Cavity Flow	4
III. Experimental Equipment	9
Water Table Apparatus	9
Water Table	9
Nozzles	9
Cavity Models	11
Air Flow Apparatus	11
Test Section Assembly	11
Air Supply System	14
IV. Experimental Procedures	16
Water Table Tests	16
Froude Number Determination	16
Velocity Measurements	20
Depth Measurements	20
Flow Visualization	21
Air Test Procedures	22
Pressure Measurements	22
Flow Visualization	22
V. Results and Discussion	26
Water Table Results	26
Flow Visualization	26
Effectiveness of Suppression Methods	29
Air Flow Results	32
Comparison to Other Investigations	33
Oscillation Reduction Effectiveness	37

VI. Conclusions	56
VII. Recommendations	58
Bibliography	59
Vita	60

List of Figures

<u>Figure</u>		<u>Page</u>
1	Cavity Geometry Nomenclature	3
2	Two-Dimensional Open Cavity Flow	5
3	Two-Dimensional Closed Cavity Flow	5
4	Shear Layer Oscillation in an Empty Rectangular Cavity	8
5	Water Table Schematic	10
6	Water Table Test Setup	12
7	Photograph of Air Flow Test Section Assembly	13
8	Photograph of Test Assembly on Calming Chamber	15
9	Geometric Cavity Shapes - Tested on the Water Table	17
10	Cavities with Suppression Devices - Tested on the Water Table	18
11	Double Cavity Configurations - Tested on the Water Table	19
12	Cavity Configurations - Tested in Supersonic Flow	23
13	Schematic of Schlieren Setup	24
14	Stages of a Typical Oscillation Cycle for Flow Over an Empty Rectangular Cavity on the Water Table	27
15	Vortex Interaction with Shear Layer for Subsonic Flow	30
16	Nondimensional Resonant Frequencies as a Function of Mach Number with Implementation of Rossiter's Formula	35
17	Nondimensional Resonant Frequencies as a Function of Mach Number with Implementation of Modified Rossiter Formula	36

<u>Figure</u>		<u>Page</u>
18	Schlieren Photographs - Shear Layer above (a) Rectangular Cavity; (b) Ramped Cavity; $M = 1.6$; $L/D = 2$. . .	38
19	Narrow Band Spectra - (a) Rectangular Cavity; (b) Ramped Cavity; $M = 1.6$; $L/D = 2$	39
20	Schlieren Photographs - Shear Layer above (a) Rectangular Cavity; (b) Ramped Cavity; $M = 1.9$; $L/D = 2$. . .	40
21	Narrow Band Spectra - (a) Rectangular Cavity; (b) Ramped Cavity; $M = 1.9$; $L/D = 2$	41
22	Schlieren Photographs - Shear Layer above (a) Rectangular Cavity; (b) Ramped Cavity; $M = 1.6$; $L/D = 4.25$. . .	43
23	Narrow Bank Spectra - (a) Rectangular Cavity; (b) Ramped Cavity; $M = 1.6$; $L/D = 4.25$	44
24	Schlieren Photographs - Rectangular Cavity with Leading Edge Ramp; $M = 1.6$; (a) $L/D = 1.6$; (b) $L/D = 2.4$; (c) $L/D = 1.9$; (d) $L/D = 2.8$	45
25	Narrow Band Spectra - Rectangular Cavity with Leading Edge Ramp; $M = 1.6$; (a) $L/D = 1.6$; (b) $L/D = 2.4$; (c) $L/D = 1.9$; (d) $L/D = 2.8$	46
26	Narrow Band Spectra - Double Rectangular Cavities - (a) Forward Cavity; (b) Rear Cavity; Single Rectangular Cavity; $M = 1.6$; $L/D = 2$. . .	48
27	Schlieren Photographs - Double Cavities - (a) Rectangular; (b) Ramped; $M = 1.6$; $L/D = 2$	49
28	Schlieren Photographs - Double Cavities - (a) Rectangular; (b) Ramped; $M = 1.9$; $L/D = 2$	50

<u>Figure</u>		<u>Page</u>
29	Narrow Band Spectra - Double Cavities - (a) Forward Rectangular Cavity; (b) Forward Ramped Cavity; (c) Rear Rectangular Cavity; (d) Rear Ramped Cavity; $M = 1.6$; $L/D = 2$	51
30	Narrow Band Spectra - Double Cavities - (a) Forward Rectangular Cavity; (b) Forward Ramped Cavity; (c) Rear Rectangular Cavity; (d) Rear Ramped Cavity; $M = 1.9$; $L/D = 2$	52

List of Tables

<u>Table</u>		<u>Page</u>
I	Rectangular Cavity Dynamic Response Data	34
II	Mode Frequency Amplitudes for Single Cavity Configurations	54
III	Mode Frequency Amplitudes for Double Cavity Configurations	55

List of Symbols

<u>Symbol</u>	<u>Definition</u>
D	Cavity Depth, ft
F	Froude Number, $V/\sqrt{g h}$
f	Frequency, Hz
g	Acceleration of Gravity, ft/sec^2
h	Water Depth, ft
k	Adiabatic Exponent
L	Cavity Length, ft
M	Mach Number, U/a_∞
m	Integer
S	Strouhal Number, $\frac{fL}{U} = \frac{m - 0.25}{M + 1.75}$
S*	Modified Strouhal Number, $\frac{fL}{U} = \frac{m - 0.25}{\frac{M}{(1 + .2M^2)^{1/2}} + 1.75}$
P_0	Freestream Stagnation Pressure, psi
P_{rms}	rms Fluctuating Pressure, psi
U	Freestream Velocity, ft/sec
V	Freestream Velocity, ft/sec
μ	Mach Angle, rad

Abstract

An experimental study was undertaken to investigate the use of a water table to define the parameters that influence the pressure oscillations resulting from air flow over open cavities. Tests were also conducted to investigate means to eliminate or reduce these oscillations.

High-speed motion pictures of the flow over cavities on the water table provided a record of the sequence of events which occurred during a typical oscillation cycle. A comparison of these events with events derived from air studies showed that the water table can be used to predict the response of cavities to air flow over them.

The water table tests clearly showed that the transverse oscillations of the shear layer are related to the cavity oscillations. Various cavity geometries were tested on the water table for Froude numbers from 0.6 to 3.3 in an attempt to find those configurations which reduce oscillations.

The configurations which showed the greatest reduction in oscillations on the water table were investigated in a supersonic free air jet. Dynamic pressure recordings and schlieren photographs were obtained for these tests. A narrow band analysis of the pressure recordings was conducted and a plot of amplitude vs. frequency, was made. A comparison of these plots with corresponding schlieren

photographs again showed that a cavity with a nonoscillating shear layer produced no discrete pressure oscillations within it.

AN EXPERIMENTAL INVESTIGATION OF
OPEN CAVITY PRESSURE OSCILLATIONS

I. Introduction

Background

Air flow over open aircraft bays causes a strong interaction between the free stream and the fluid within the cavity producing pressure oscillations in the bay. These pressure oscillations can be of such high intensity that they can excite vibrations in the aircraft structure and bay contents which may result in structural and equipment failure; premature store release; unpredictable inputs at store release, resulting in potentially dangerous separation characteristics and trajectory error; and crew discomfort and performance degradation.

In the past, numerous theoretical and wind tunnel investigations of pressure oscillations in open cavities have been undertaken (Ref 1-5). These investigations have led to a reasonable understanding of the mechanisms likely to cause oscillations and to semi-empirical schemes that predict resonant frequencies with satisfactory accuracy. To date, however, the complete solution to the intricate flow mechanisms about and within an open cavity is poorly understood. A result of this lack of understanding is the inability to formulate detailed design criteria for cavities or for the aerodynamic mechanisms that would eliminate or reduce cavity pressure oscillations.

Objective

The purpose of this study is to use water table flow visualization to define the parameters that influence the pressure oscillations which occur in open cavities and to investigate (both on the water table and in air flow) means to eliminate or reduce these oscillations.

Scope

High speed motion pictures (factor 2:1) of the flow over cavities on the water table are used to define the parameters that influence cavity oscillations and to investigate the influence of changes in cavity geometry on the oscillations within the cavity. The flow over two closely spaced cavities, one immediately behind the other, is also investigated. The cavities considered in this study are represented by two-dimensional cutouts, Fig. 1, with length-to-depth ratios (L/D) from one to four. The Mach numbers investigated range from 0.6 to 3.3.

Several configurations, shown on the water table to reduce oscillations, are tested in supersonic air flow. Schlieren photographs and dynamic pressure measurements are obtained for these configurations and compared with similar results obtained for rectangular cavities.

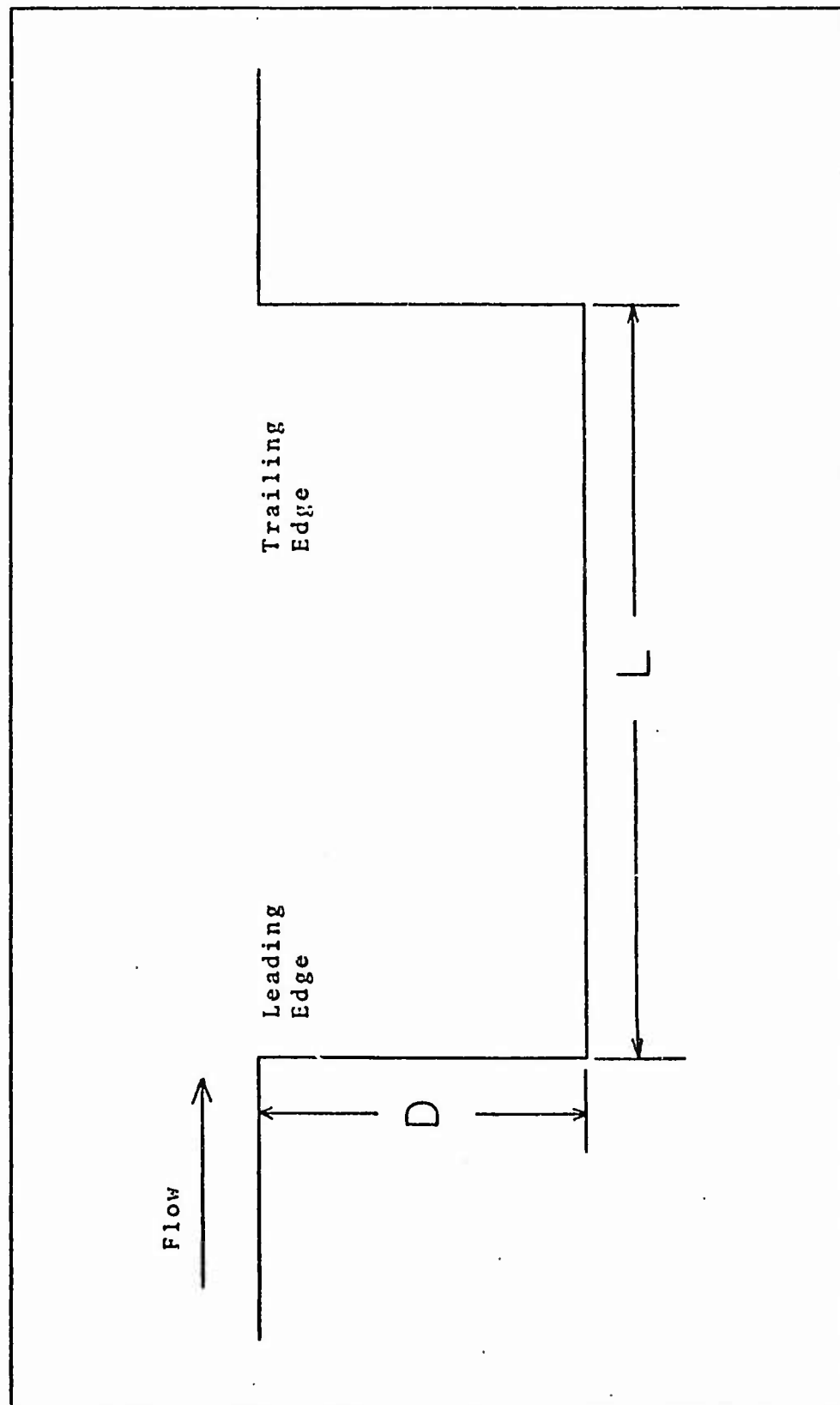


Fig. 1. Cavity Geometry Nomenclature.

II. Discussion of Cavity Flow

The problem of flow within open cavities can be viewed as two-dimensional. Previous studies have shown that spanwise flow has no significant influence on cavity oscillations (Ref 3:2; 5:2189). The freestream flow direction dominates the internal flow so strongly that three-dimensional effects are restricted to perturbations in the dominant two-dimensional flow directions. Rosko found the main effect of finite span to be that the vorticity, which is trapped within the cavity in two-dimensional flow, can escape along the ends into a trailing vortex system in three dimensions (Ref 4:10). Maull and East found that deep cavities ($L/D < 1$) did possess periodic flow patterns in the spanwise direction, but that these tended to decrease with increasing freestream velocity (Ref 6:623). Since the present study is not concerned with deep cavities, the assumption of two-dimensional cavity flow is adequate.

Because of the sharpness of the corner, flow separation occurs at the leading edge of the cavity, which forms a shear layer between the high speed flow outside the cavity and the relatively slow eddying flow within the cavity. This is shown in Fig. 2. The shear layer either spans the cavity or reattaches to the cavity floor (Ref 5:258). Cavities in which the shear layer spans the gap and reattaches to the downstream edge are termed open cavities. Figure 2 shows a schematic of an open cavity. A cavity in which the shear

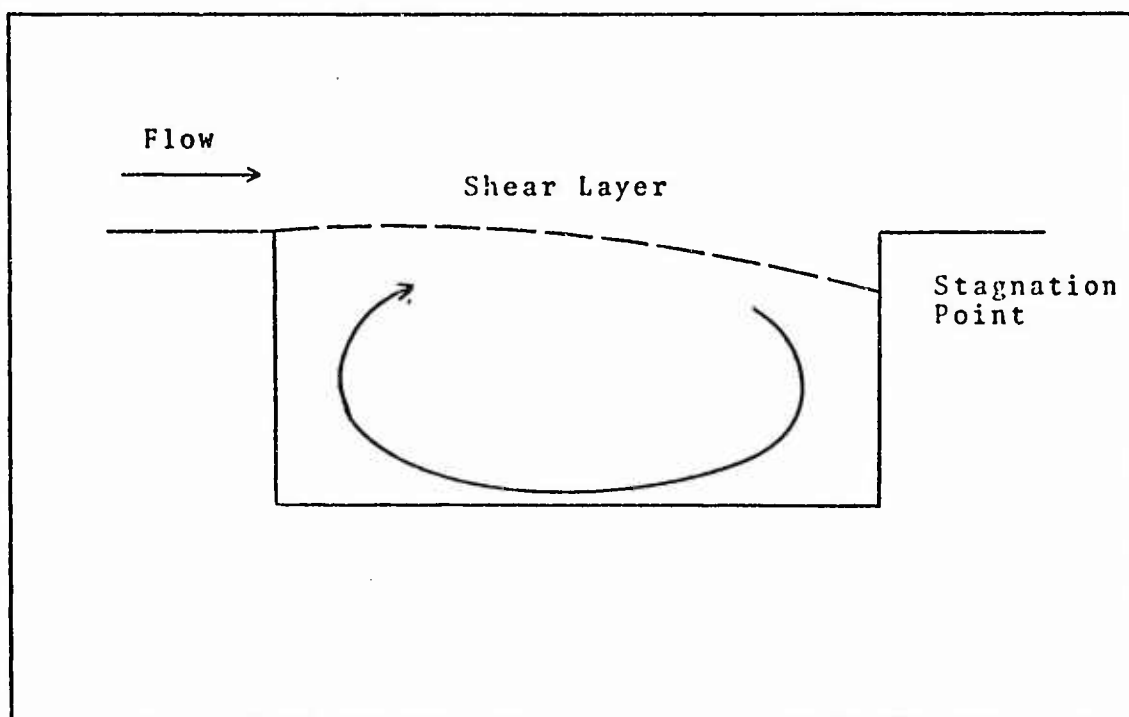


Fig. 2. Two-Dimensional Open Cavity Flow.

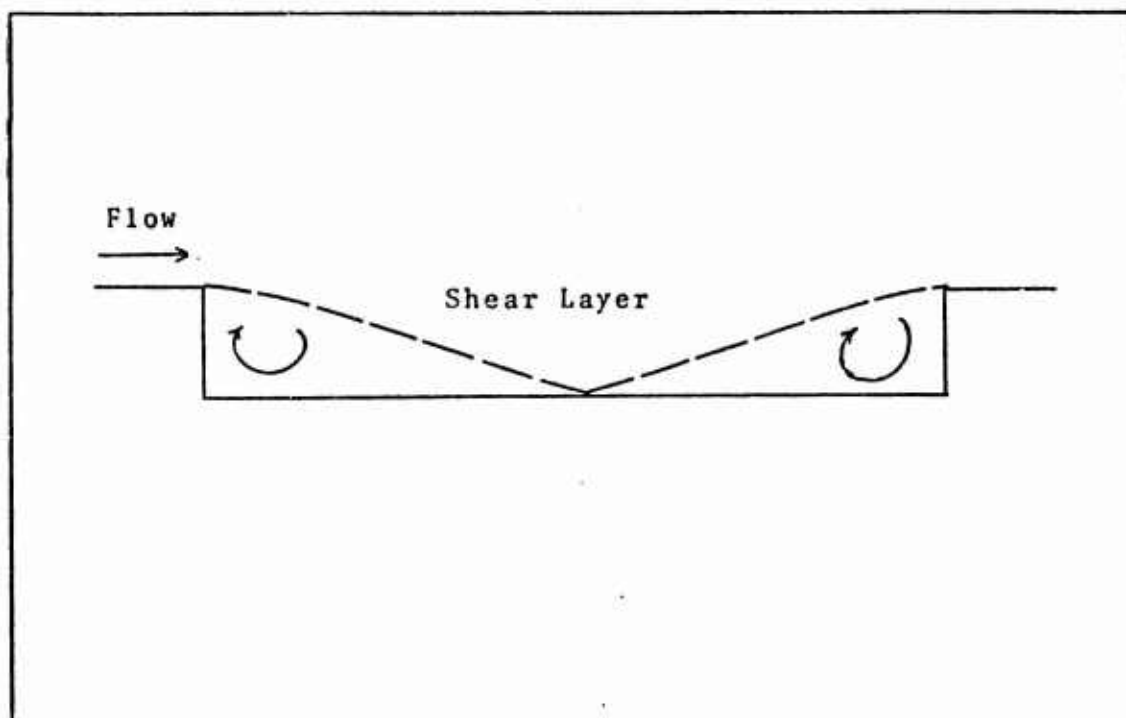


Fig. 3. Two-Dimensional Closed Cavity Flow.

layer reattaches to the cavity floor, shown in Fig. 3, is termed a closed cavity and occurs when L/D is greater than seven. The unsteadiness associated with this flow pattern is predominantly random and does not exhibit periodic pressure oscillations. Therefore this configuration was not considered in the present study.

The unsteadiness associated with the shear layer over an open cavity results in pressure oscillations within the cavity. In laminar flow the shear layer unsteadiness results in a periodic shedding of discrete vortices from the leading edge of the cavity, while in turbulent flow it results in random fluctuations in the shear layer (Ref 1:8). Karamcheti has shown that an approaching laminar boundary layer is capable of initiating very powerful oscillations that exceed those resulting from a turbulent boundary layer for otherwise identical conditions (Ref 1:5).

Heller, Holmes, and Covert have investigated the possible resonance modes and frequencies in open cavities (Ref 2). This investigation showed that in deep ($L/D < 1$) cavities the resonance mode is usually in the depth direction, that is, the cavity responds like an ordinary acoustic resonator. For shallow ($L/D > 1$) cavities the resonance mode is in the streamwise direction of the cavity (Ref 2:2).

Heller, et al. also found that although the vortices shed from the upstream edge of the cavity are the primary component of the resonance excitation mechanism, the downstream edge of the cavity plays a role in governing the

strength of the oscillations (Ref 2:25). The physical mechanism involved is shown in Fig. 4. As the shear layer oscillates, it is periodically swallowed into the cavity at the rear lip and disgorged again. A stagnation point is created inside the rear lip each time the shear layer is swallowed. Also fluid is injected into the cavity and the local pressure increases. When the shear layer is disgorged, the pressure drops to a value near the freestream value as the fluid is vented into the freestream. With each pressure oscillation at the rear lip, a compression wave is set into motion in the upstream direction as shown in Fig. 4.

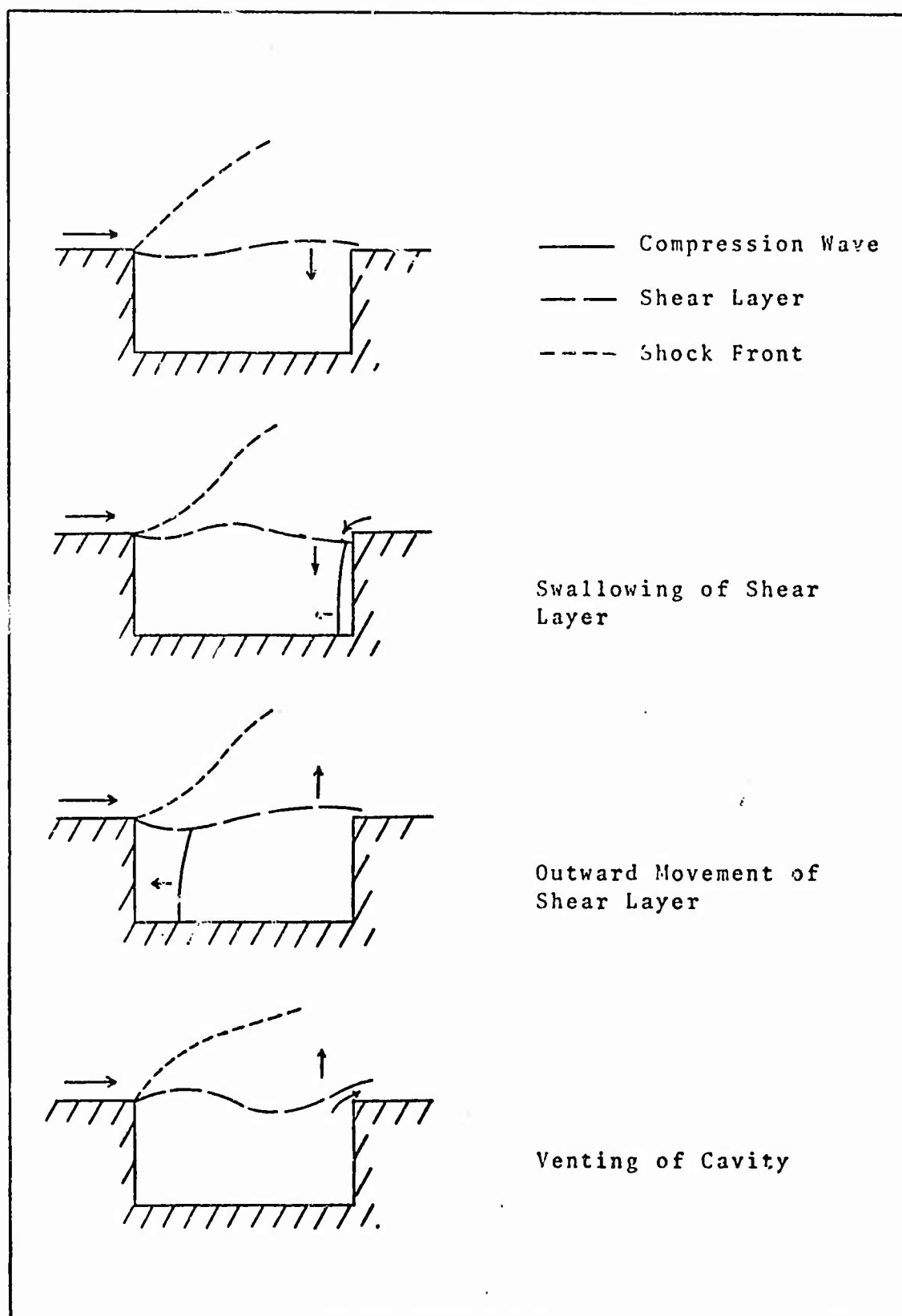


Fig. 4. Shear Layer Oscillation in an Empty Rectangular Cavity.

III. Experimental Equipment

Water Table Apparatus

The experimental apparatus used in the water table study consisted of the water table, nozzles, and cavity models.

Water Table. Figure 5 shows a schematic of the water table used in this study. It consists primarily of a large horizontal glass floor, 8 ft long and 4 ft wide; an upstream accumulator tank; and a circulating pump isolated from the table to minimize vibrations.

During operation of the table, water is pumped from the reservoir tank into the accumulator tank producing a shallow sheet of water that flows over the test area under the influence of gravity. As the water leaves the accumulator tank, it passes through a cloth filter to remove impurities and through a metal screen to establish a uniform velocity profile. A weir is provided at the foot of the test area to control the water depth. Water is recirculated at a maximum rate of 36 gal/min. The pump output is controlled by a series of valves between the pump and the accumulator tank.

Nozzles. Four different two-dimensional nozzles were used in the water table study. The nozzles included one subsonic convergent conical nozzle and three supersonic convergent-divergent laval nozzles which provided Froude numbers of 1.6, 2.3 and 3.3.

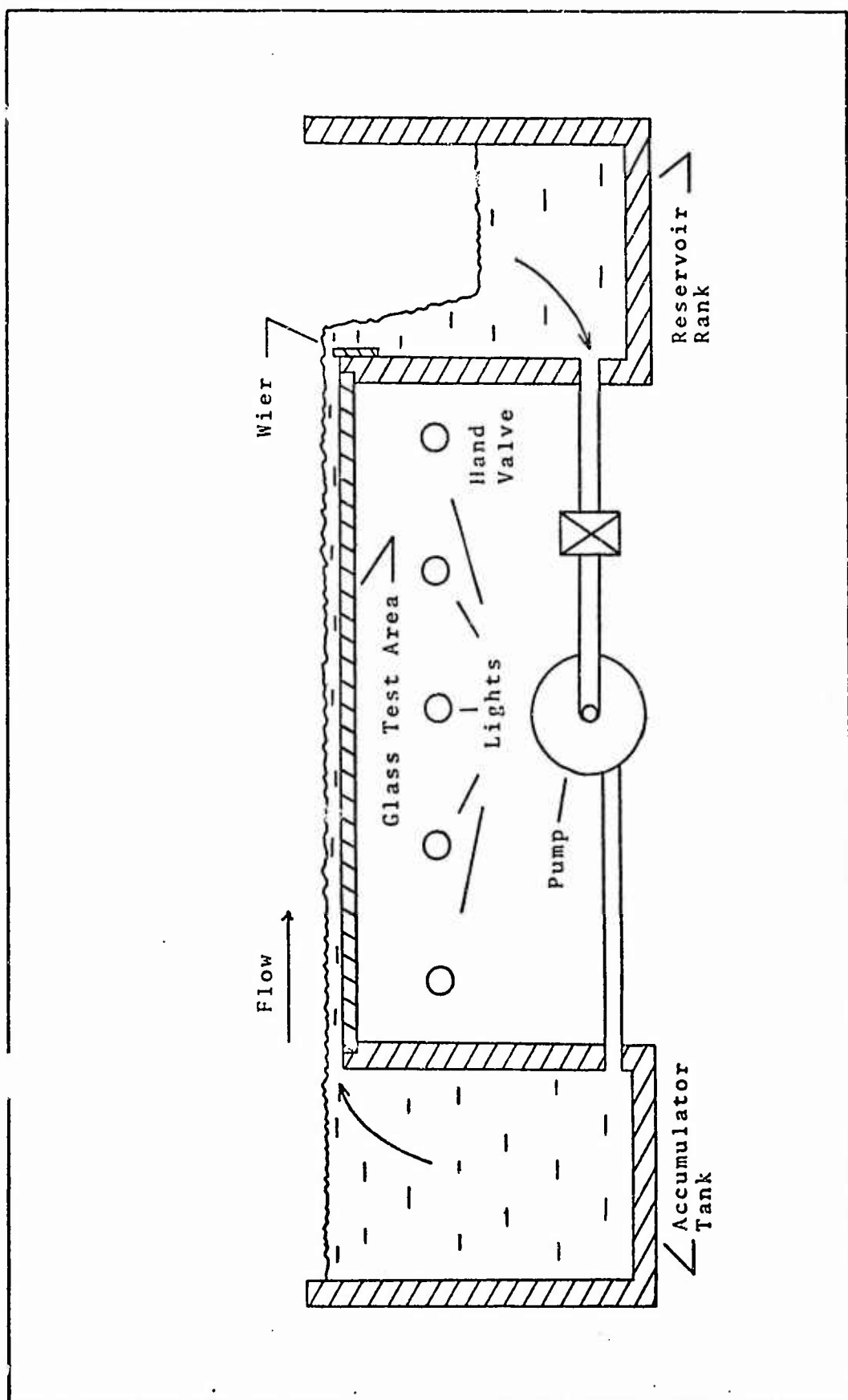


Fig. 5. Water Table Schematic.

The nozzles were constructed from 1 7/8 in thick pine and coated with varnish to protect them from exposure to the water. The shapes of the Laval nozzles were determined by a computer program written by Major C. G. Stolberg of the Aero-Mechanical Department, AFIT. This program uses isentropic relationships and the method of characteristics with $k = 2.0$ to design the nozzle shapes.

Cavity Models. The cavity models used on the water table were made by positioning pieces of wood at the end of the nozzle as shown in Fig. 6. The wood pieces used were 1 1/2 in thick and 3 1/2 in wide. Changes in the length of the cavity were made by repositioning the piece of wood forming the rear wall of the cavity. The cavity depth measurement was maintained at 3 1/2 in for all cavity configurations investigated. Changes in the cavity geometry were made by inserting wooden blocks of the desired shape.

Air Flow Apparatus

The experimental equipment used in the air flow study consisted of the test section assembly and the air supply system.

Test Section Assembly. The test section assembly, shown in Fig. 7, consisted of a two-dimensional Laval nozzle and the cavity model sandwiched between two pieces of 3/4 in clear plexiglass. Paper gasket material was installed between the nozzles and cavity models and the plexiglass to provide an air-tight seal.

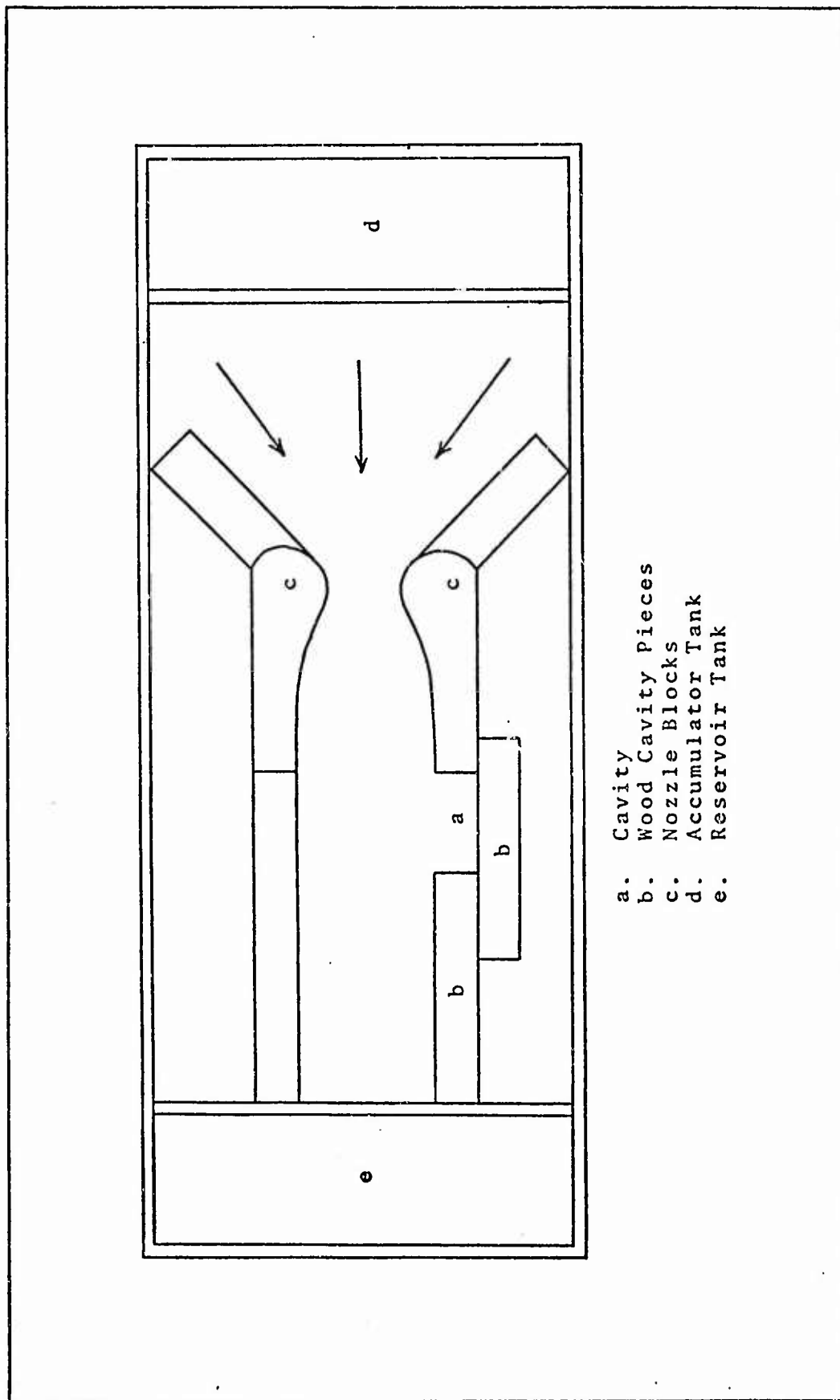


Fig. 6. Water Table Test Setup.

Reproduced from
best available copy.

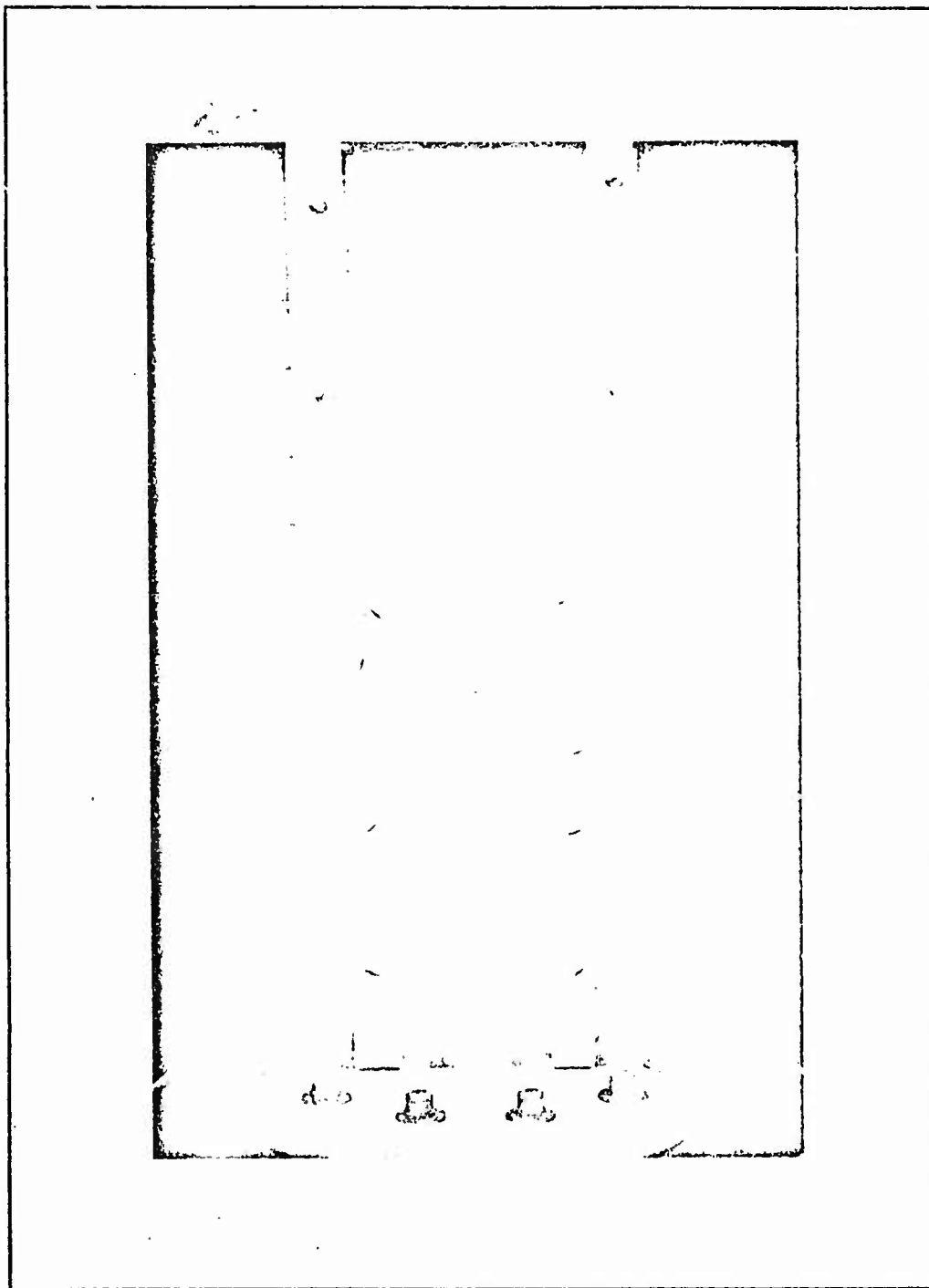


Fig. 7. Photograph of Air Flow Test Section Assembly.

Two sets of two-dimensional Laval nozzles, constructed from 5/8 in brass, provided Mach numbers of 1.7 and 2.3 at the nozzle exit.

The cavities used in the air flow study were constructed from 5/8 in thick aluminum. All cavities had a depth of 1 in. Interchangeable parts allowed lengths of 2 in and 4 1/4 in. The cavity leading edge was located 2 in downstream from the nozzle exit.

Threaded holes, into which microphones were screwed, were provided in one piece of plexiglass. The locations of these holes are shown in Fig. 10.

Air Supply System. Compressed air was supplied to the cavity model by a compressor capable of delivering continuous air flow at approximately 100 psi. The test section assembly was positioned on top of a calming chamber as shown in Fig. 8.

Reproduced from
best available copy.

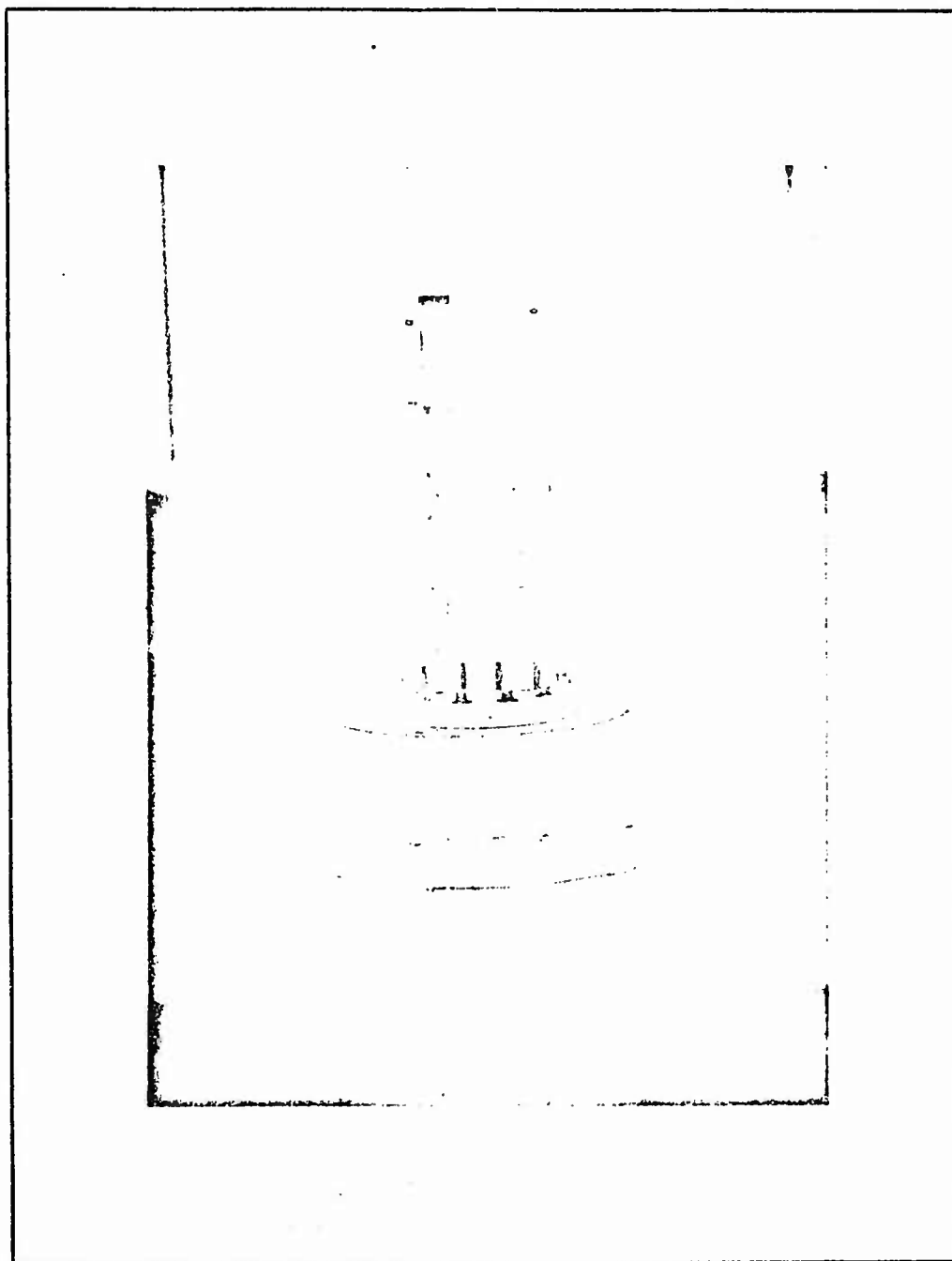


Fig. 8. Photograph of Test Assembly on Calming Chamber.

IV. Experimental ProceduresWater Table Tests

A typical test on the water table involved positioning the desired nozzle and cavity model as shown in Fig. 6, determining the Froude number at the nozzle exit, and taking motion pictures of the flow field within and above the cavity. After motion pictures were taken of all the cavity configurations at a given Froude number, a different nozzle was positioned on the water table, a new Froude number determined, and the flow over each cavity was again filmed. In this manner a film record of the flow over all of the cavity configurations at each of the Froude numbers was made. Figures 9, 10, and 11 show schematics of the various cavity configurations investigated on the water table.

Froude Number Determination. The Froude number on the water table corresponds to the Mach number in air. Before each series of tests on the water table, the Froude number at the nozzle exit was determined using the following equations (Ref 7:5):

$$F_1 = \frac{V_1}{\sqrt{gh_1}}$$

$$h_0 = h_1 [(F_1^2/2) + 1] \quad (2)$$

$$F_2 = \sqrt{2} [(h_0/h_2) - 1]^{1/2} \quad (3)$$

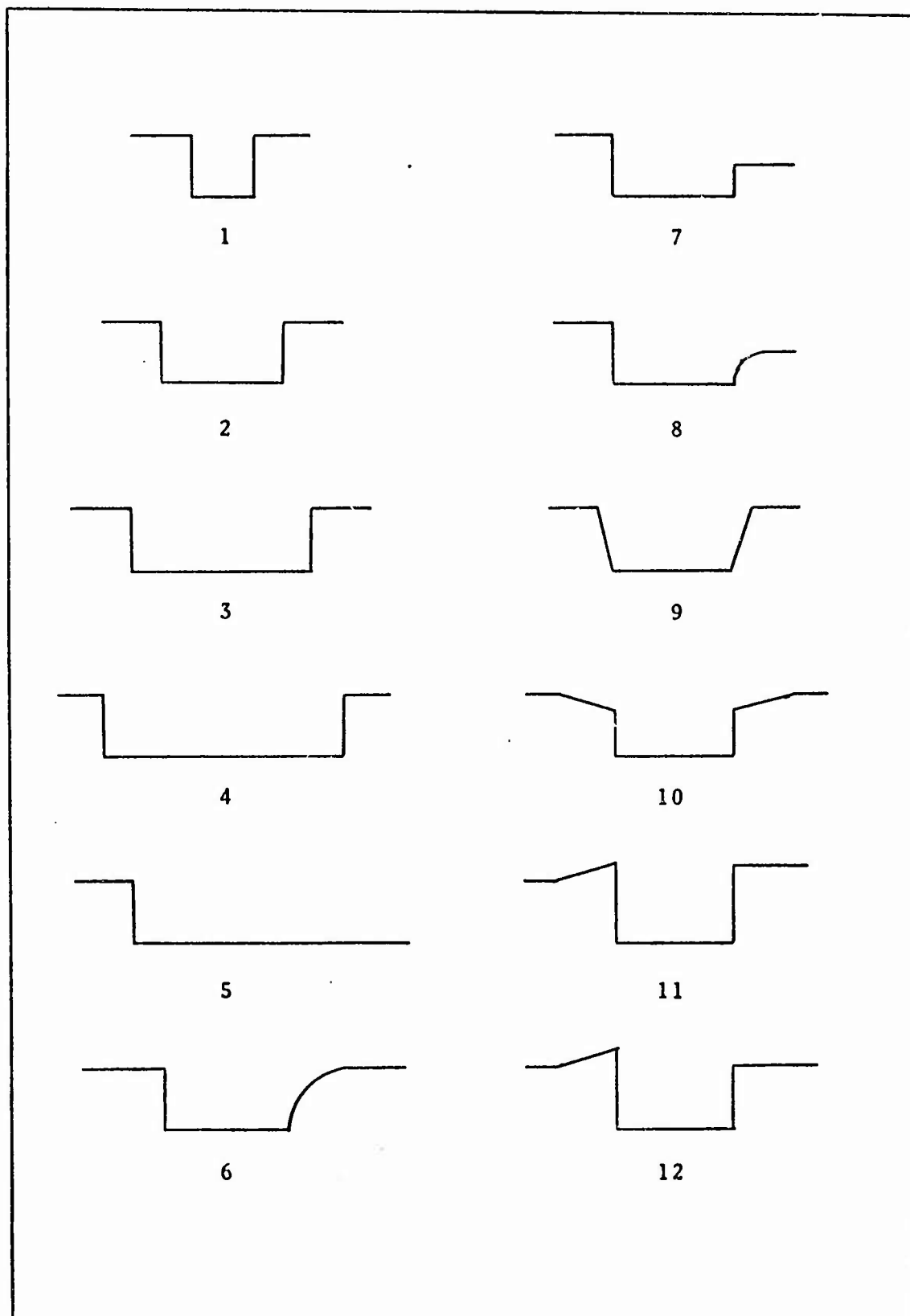


Fig. 9. Geometric Cavity Shapes - Tested on the Water Table.

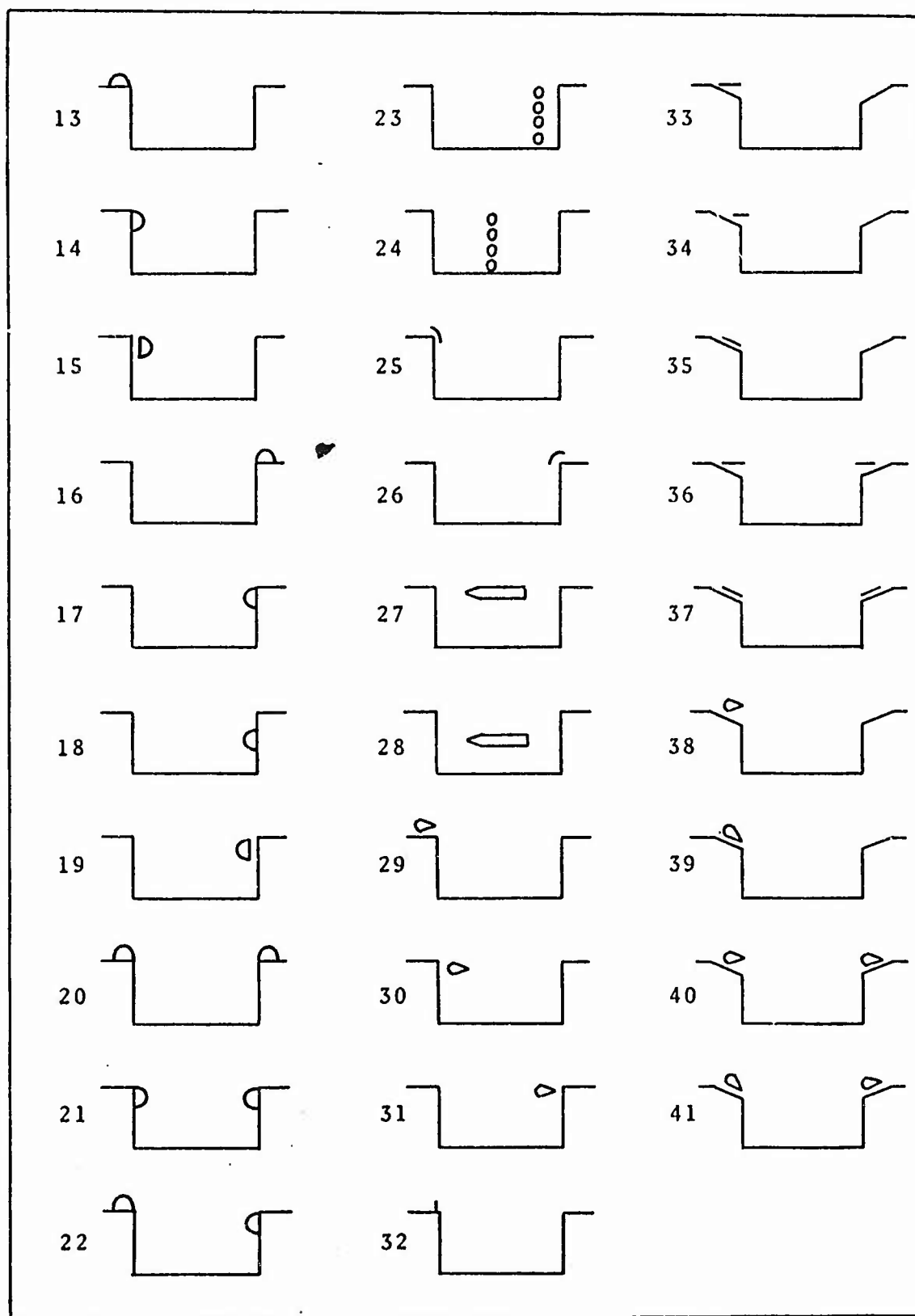


Fig. 10. Cavities with Suppression Devices - Tested on the Water Table.

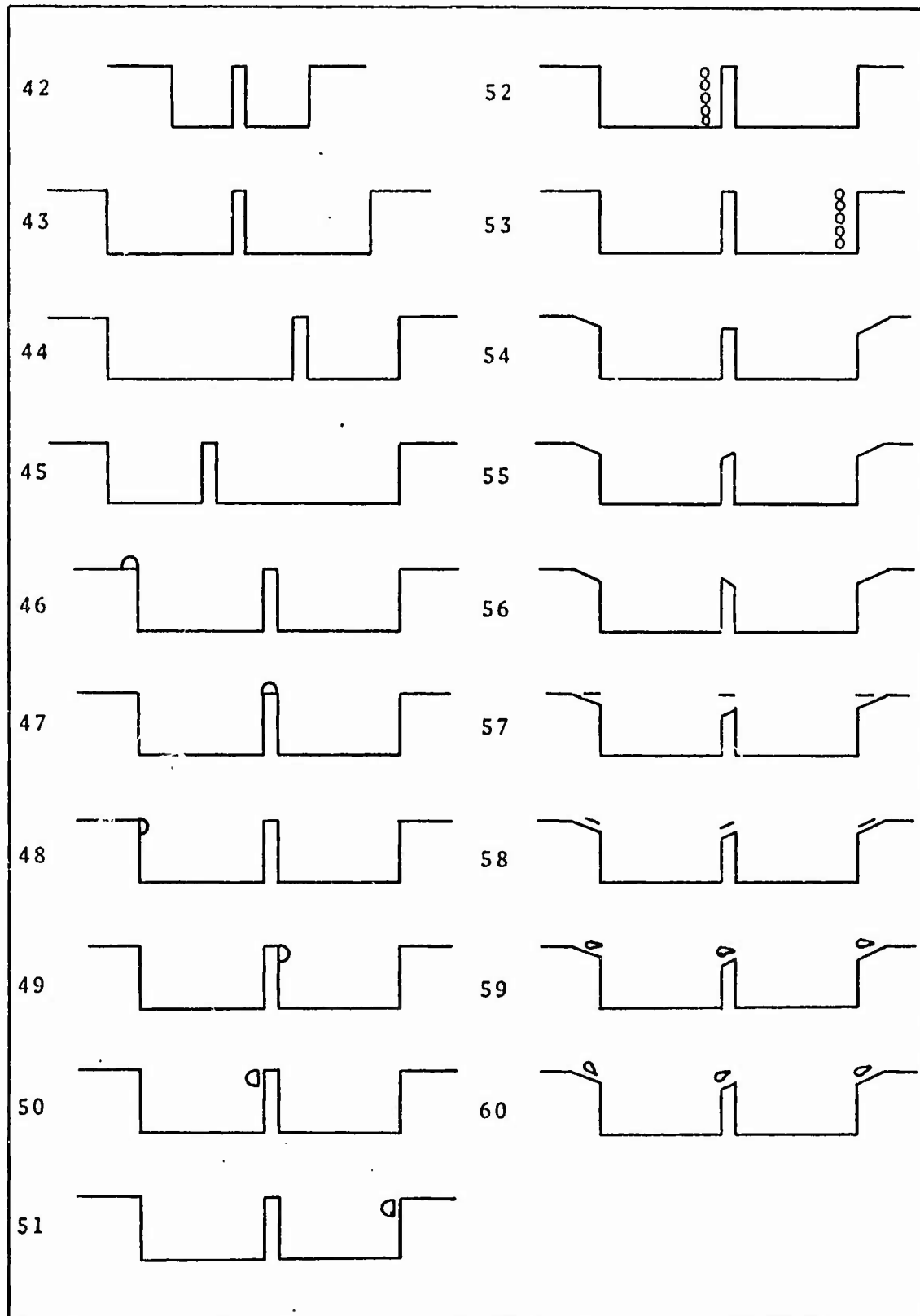


Fig. 11. Double Cavity Configurations - Tested on the Water Table.

In these equations, subscript 0 refers to stagnation conditions, subscript 1 refers to the region upstream from the nozzles, and subscript 2 refers to the position at which the Froude number is desired.

A Froude number for supersonic flow was determined by measuring the water depth and velocity upstream of the nozzles and the water depth at the nozzle exit. With this information, the above equations were solved for F_2 .

A Froude number for subsonic flow was determined by measuring the local water depth and velocity and solving Eq (1).

Velocity Measurements. The water velocity was measured by timing a small piece of wood as it traveled on the water between two lines 12 inches apart. The piece of wood was timed a minimum of five times and the times averaged to determine the velocity.

An electric timer graduated every 0.01 second was used for these measurements. With this timer, measurements to the nearest 0.005 second were possible.

Depth Measurements. A depth gauge constructed from a traversing mechanism produced by Tropel, Inc., was used to obtain depth measurements. The traversing mechanism contains a slide that is moved by rotating a knob at the top. The slide moves one inch for every 20 turns of the knob. A thin steel rod is attached to the slide. The gauge was mounted on a beam that spans the water table.

A depth measurement was made by turning the knob until the steel rod touched the water surface and then counting the turns until the rod touched the table surface. Depth measurements to within 0.004 in were possible.

Flow Visualization. Two methods were used to visualize the flow phenomena during the water table testing. The first method employed dye injection; the second method used motion pictures.

Dye injection was used as the primary means of visualizing the shear layer reaction over the cavities. The dye was injected into the boundary layer ahead of the cavity using medical syringes and hypodermic needles. Writing ink diluted with water was used as the dye.

Motion pictures were the primary means of visualizing the oscillations within the cavity. The movies were taken at 48 frames per second with a variable speed movie camera. The camera was mounted above the water table directly over the cavity. Light was provided by a single flood light positioned at a 45 degree angle to the water surface and a 45 degree angle to the freestream velocity.

The movies were analyzed using a variable speed projector which allowed film speeds from 800 to 1500 frames per minute. In addition, the projector could be hand cranked for single frame viewing.

Air Test Procedures

For a typical air flow test, the desired cavity configuration and nozzle were fitted into the test section assembly and the assembly mounted on the top of the calming chamber. The air was turned on and the pressure was allowed to stabilize. When the system was stable, a one minute recording was made of the dynamic pressure. While the recording was being made a schlieren photograph of the flow field in and above the cavity was made. Cavity configurations which were investigated in air flow are shown in Fig. 12.

Pressure Measurements. Dynamic pressure information was sensed by three Model 376 Dynamic Pressure Transducers made by Bolt, Beranek, and Newman, Inc. This information was recorded on a Leach portable tape recorder with a frequency range of 0 - 10 KHz. A narrow band analysis of the recordings provided a plot of amplitude vs. frequency for the dynamic pressure in each cavity tested.

Flow Visualization. A high speed schlieren optical system was used to obtain still photographs of each test. The photographs were taken using a 1/6 microsecond spark lamp. Figure 13 is a schematic of the schlieren setup.

Besides serving as a record of the flow over the cavity, the photographs were used to determine the Mach number of the flow over the cavity. The Mach number was determined by measuring the Mach angle at the leading edge of the cavity

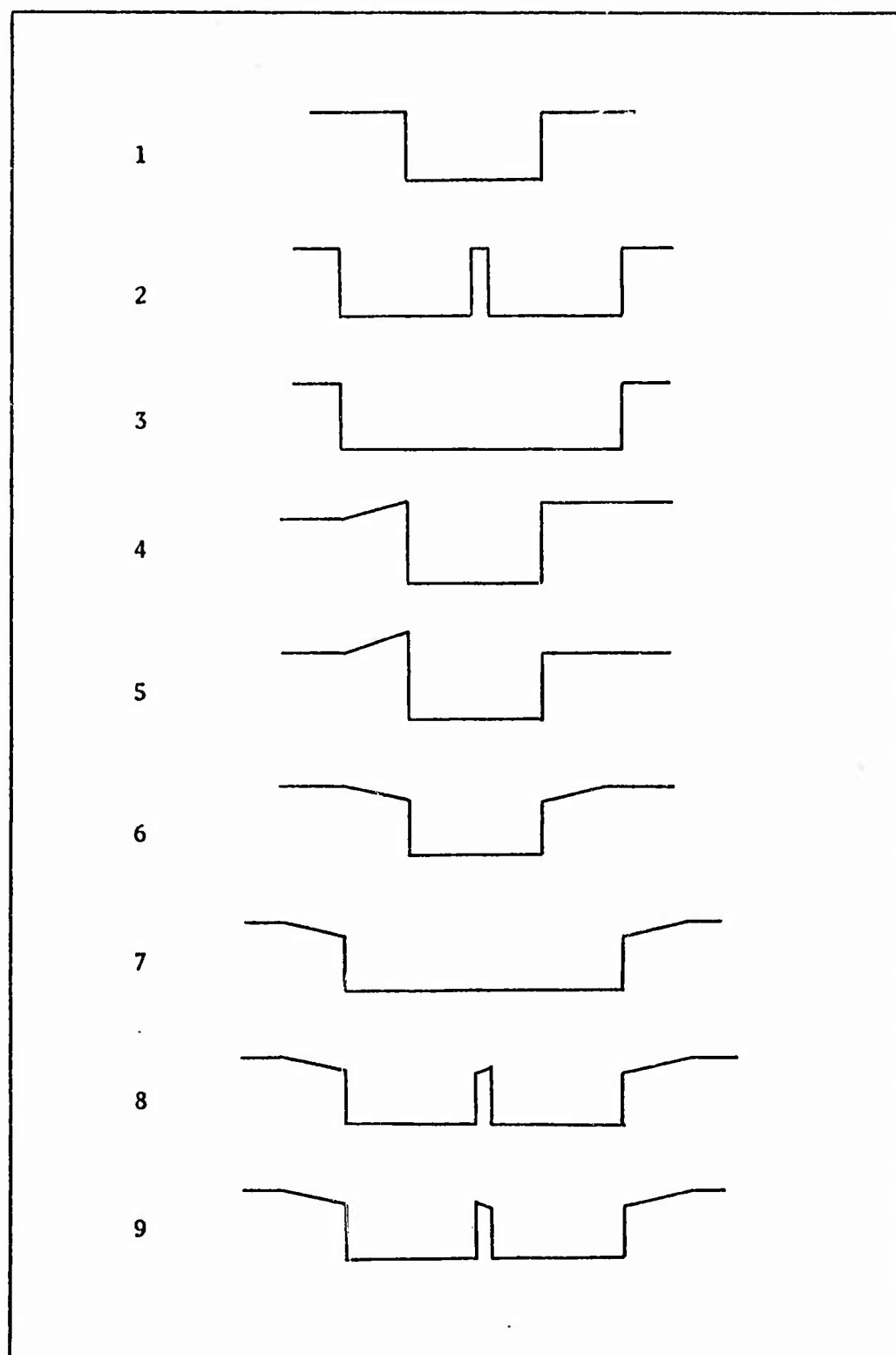


Fig. 12. Cavity Configurations - Tested in Supersonic Flow.

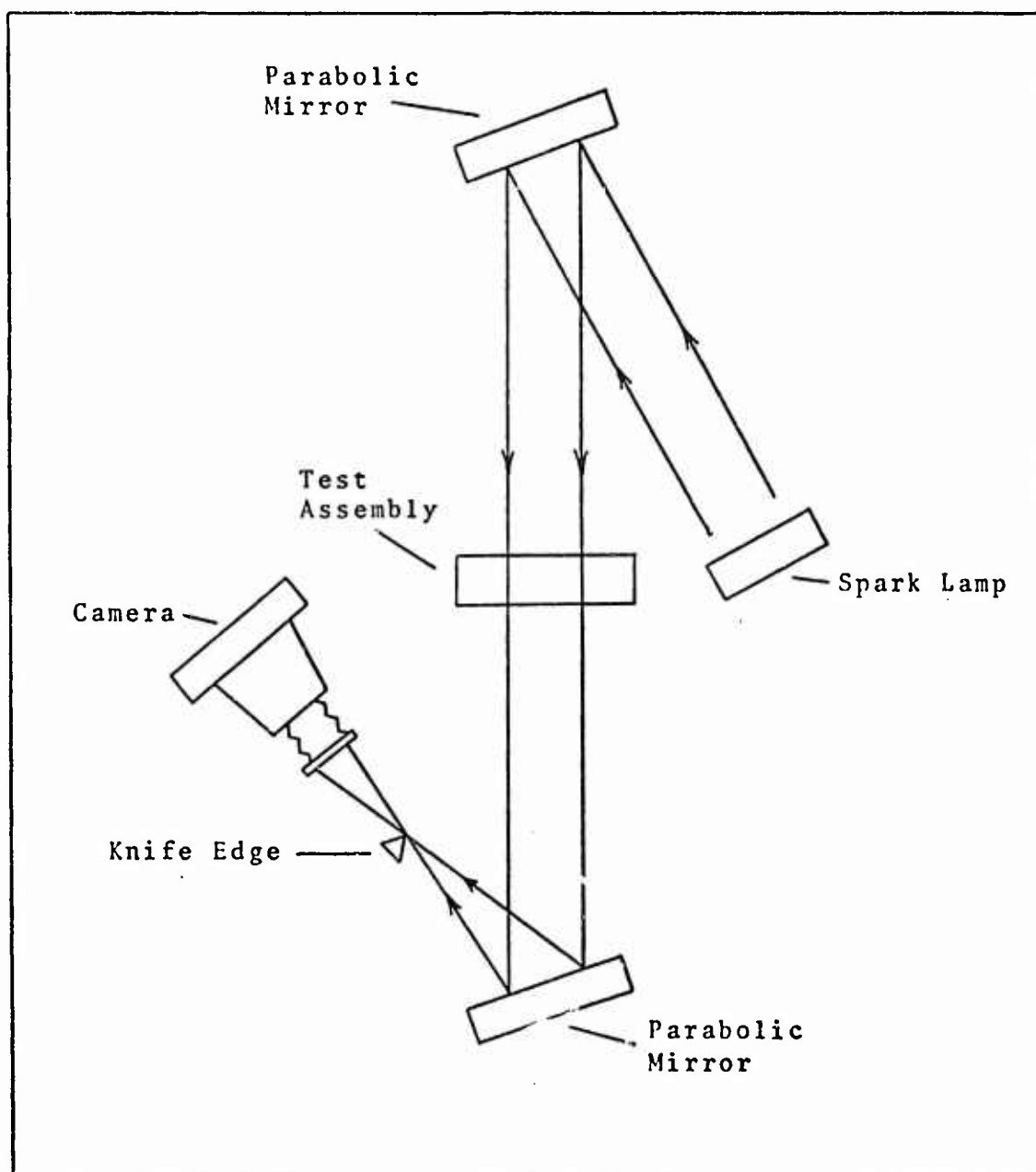


Fig. 13. Schematic of Schlieren Setup.

and converting this to Mach number through the relation

$$\mu = \sin^{-1} \frac{1}{M} \quad (4)$$

where μ is the Mach angle.

V. Results and Discussion

The main objectives of this investigation were to determine if water table flow visualization could be used to represent the phenomena associated with air flow over open cavities, and to investigate ways to eliminate or reduce pressure oscillations within cavities.

Water Table Results

Flow Visualization. Motion pictures of the flow over cavities on the water table provide a means to study in detail a typical oscillation cycle within the cavity. Figure 14 is a series of sketches showing the stages of such a cycle for supersonic flow. The sequence of events observed on the water table and discussed below agrees very well with the proposal put forth by Heller (Ref 2:25) and discussed in Section II of this report.

In Fig. 14(a), the shear layer is below the trailing edge of the cavity. Fluid enters the cavity at the trailing edge causing the water depth to increase and a wave to form. Through the hydraulic analogy, the square of the water depth is proportional to the pressure in air, so the increase in water depth can be related to an increase in pressure in air (Ref 8:22). Also in Fig. 14(a), the previously formed wave has moved to the front of the cavity and has reflected off the front wall.

In Fig. 14(b), the reflected wave is moving rearward with the crest of the shear layer wave. The newly formed

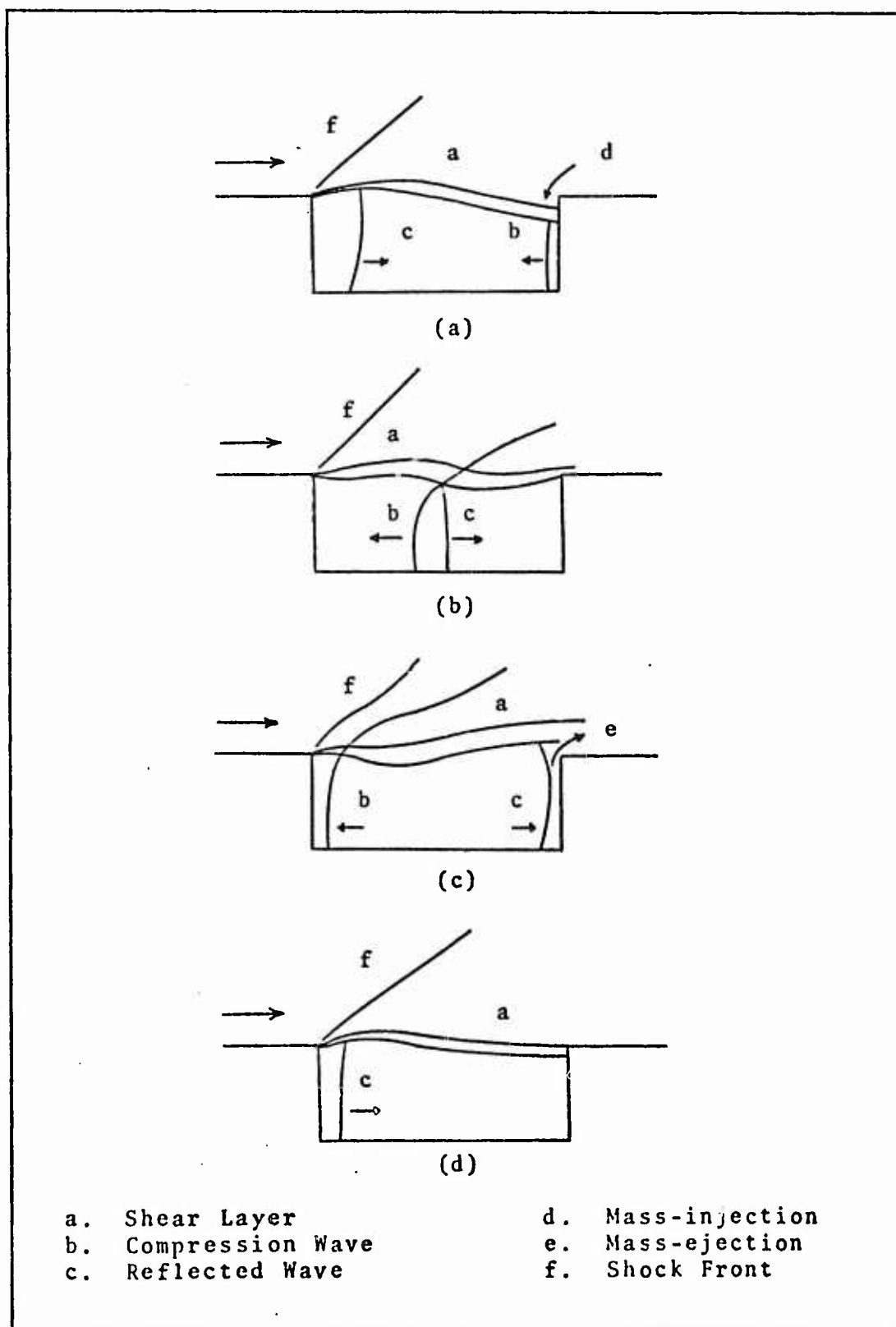


Fig. 14. Stages of a Typical Oscillation Cycle for Flow Over an Empty Rectangular Cavity on the Water Table.

wave is moving forward. These waves meet near the center of the cavity and after interacting continue in their respective directions. An oblique wave in the external flow follows the forward moving compression wave. This oblique wave could be the result of a disturbance, produced at the shear layer by the forward traveling wave, moving against the supersonic flow.

In Fig. 14(c), the forward traveling wave is approaching the front wall and the shear layer above the wave is moving out of the cavity. The reflected wave nears the rear wall and, as the shear layer goes above the trailing edge, fluid leaves the cavity at the trailing edge.

In Fig. 14(d), the trough of the shear layer wave moves toward the rear wall drawing the shear layer below the trailing edge and a new cycle begins. This sequence of events clearly associates the cavity oscillations and the behavior of the shear layer.

Several other phenomena previously observed in wind tunnel investigations were observed on the water table. Quinn found that cavity oscillation was always accompanied by the shedding of vortices from the leading edge (Ref 9:3). The movies of the water table tests showed vortices being shed in subsonic and low supersonic flow. The vortices were shed as the forward traveling wave reflected from the front wall of the cavity and they traveled across the cavity with the crest of the shear layer. At subsonic speeds the vortices

curled the shear layer so much that it "broke" as shown in Fig. 15.

East found that for any particular cavity a discrete frequency was produced over only a limited velocity range and that different frequencies occur at different velocities (Ref 10:280). This phenomenon was also seen on the water table. For example, a cavity with an $L/D = 4$ displayed no oscillations at $M = 3.3$ but showed definite oscillations at $M = 1.6$ and $M = 2.3$. In addition, the frequency of the oscillations was higher at $M = 2.3$ than at $M = 1.6$.

Finally, an investigation of two closely spaced cavities of the same size, one immediately behind the other, showed the cavities to oscillate in phase. Apparently the disturbances introduced into the flow by the upstream shear layer tend to control the phase of oscillations in the downstream cavity.

Effectiveness of Suppression Methods. The association of the shear layer behavior with the oscillations within the cavity suggests that elimination of the shear layer transverse oscillations is one means to reduce cavity oscillations. Tests on the water table showed this to be so.

Figures 9, 10, and 11 show diagrams of each of the configurations tested on the water table. For most of the configurations, the movies showed little or no change in the oscillations within the cavity compared with the oscillations in a rectangular cavity with the same L/D ratios. In

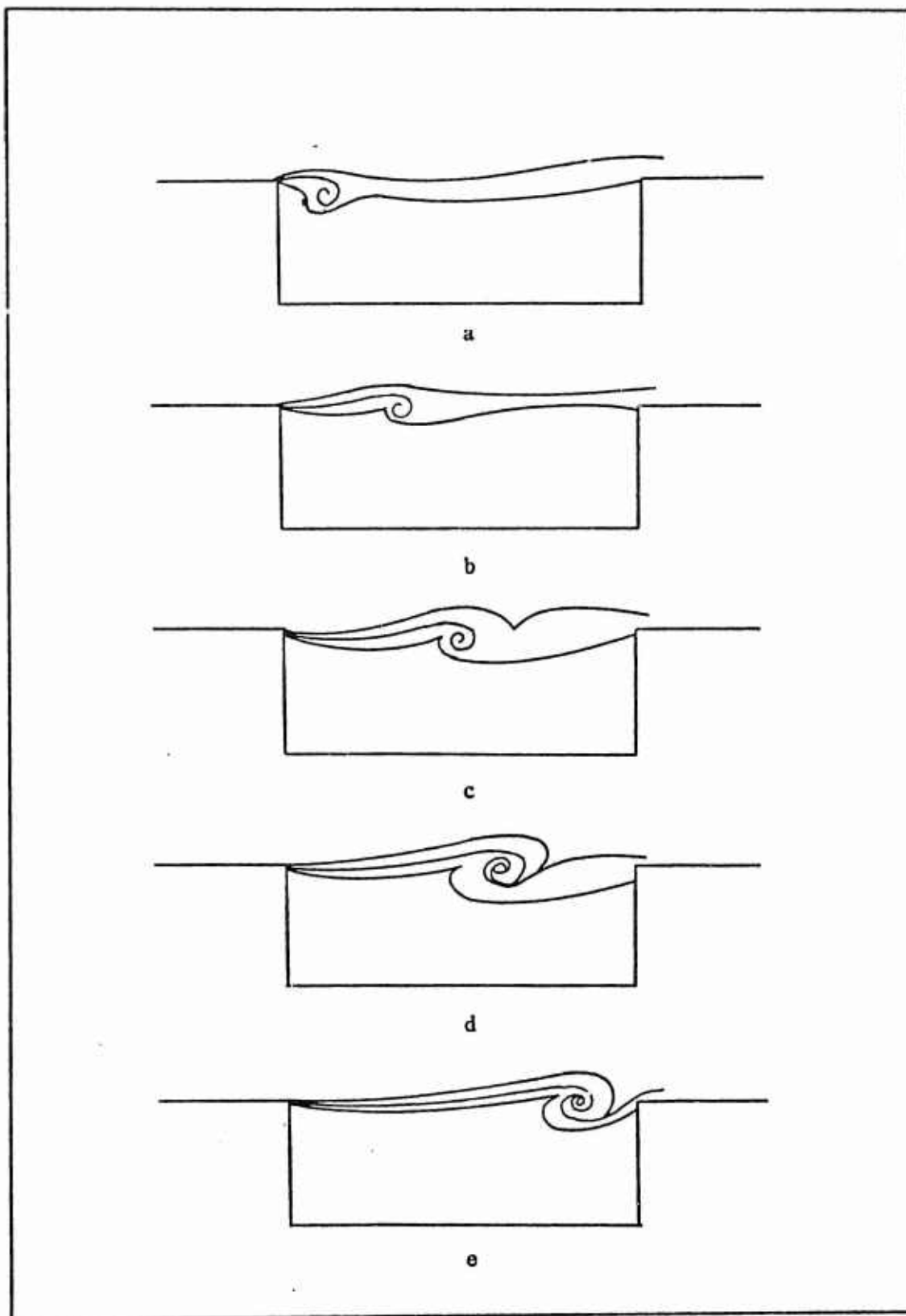


Fig. 15. Vortex Interaction with Shear Layer for Subsonic Flow.

several configurations, such as 14, 15, 21, and 30 in Fig. 10, the shear layer went deeper into the cavity causing the wave on the water table to be higher which would correspond to a higher pressure in air. In the following discussion only those configurations found most effective in reducing oscillations will be discussed.

The insertion of a vertical baffle (configuration 23, Fig. 10) just upstream of the rear wall, was found to be very effective in stopping the oscillations. As the baffle was moved near the center of the cavity, its effectiveness was diminished because oscillations developed behind it.

The insertion of a half-cylindrical cowl (configuration 19, Fig. 10) ahead of the trailing edge was effective in reducing oscillations at most Mach numbers investigated. As with the baffle, location was critical and varied with Mach number.

Stores within the cavity and touching the shear layer (configuration 27, Fig. 10) were found to be effective in stopping oscillations. If the stores were located deeper in the cavity (configuration 28, Fig. 10), however, oscillations were present above and behind the stores. The size of the stores was also critical. If the store was small compared to the length of the cavity, oscillations were present in the cavity.

A spoiler in the shape of an airfoil placed above the leading edge (configuration 29, Fig. 10) was effective in

reducing oscillations. When the spoiler was positioned at a small negative angle of attack (approximately 10°) the shear layer did not enter the cavity. Locating the spoiler in front of the trailing edge (configuration 31, Fig. 10) was more effective than the half-cylindrical cowl.

Ramps with a slope of 15 degrees leading into the cavity at the leading and trailing edges (configuration 10, Fig. 9) were very effective in reducing oscillations. The shear layer followed the ramps and showed almost no oscillation over the cavity.

A ramp with a 15 degree slope away from the cavity placed at the leading edge (configurations 11 and 12, Fig. 9) was effective in eliminating oscillations but the length of the cavity was critical. At some critical length, which depended on Mach number, the shear layer entered the cavity and oscillations were present.

When the above configurations were introduced into a double cavity system, one behind the other, oscillations were suppressed in both cavities only if the devices were applied to both cavities. Suppressing the oscillations in one cavity had no effect on the oscillations in the other cavity.

Air Flow Results

A narrow band analysis of the pressure recordings was conducted and a plot of amplitude vs. frequency was made for each configuration tested. The information from these plots

served two purposes. First, results for rectangular cavities were compared with other investigations to assure the validity of the present tests. Second, the effectiveness of the modified cavity configurations tested was determined.

Comparison to Other Investigations. The resonant frequencies corresponding to the different modes which were present in the rectangular cavities of this study are shown in Table I. Also shown in this table are the amplitudes and Strouhal numbers associated with each of these frequencies. The Strouhal numbers are plotted against Mach number in Figs. 16 and 17. Also plotted in these figures are data obtained by Rossiter and Heller (Ref 2:75).

Rossiter proposed the following empirical relationship for the Strouhal number:

$$S = \frac{fL}{U} = \frac{m - 0.25}{M + 1.75} \quad (5)$$

where m is any positive integer and corresponds to the frequency mode number (Ref 2:84). A plot of this equation as a function of Mach number is shown in Fig. 16.

Heller proposed the following modification to this equation (Ref 2:107):

$$S^* = \frac{fL}{U} = \frac{\frac{m - 0.25}{M}}{(1 + 0.2M^2)^{1/2}} + 1.75 \quad (6)$$

A plot of Eq (6) as a function of Mach number is shown in Fig. 17.

Table I
Rectangular Cavity Dynamic Response Data

	m	f, exp	dB	S, exp	f, Eq(5)	S, Eq(5)	f, Eq(6)	S*, Eq(6)
M = 1.6 L/D = 2	1	-----	---	---	2407	.22	2643	.25
	2	5600	165	.52	5617	.52	6167	.57
	3	9300	138	.86	8826	.82	9691	.90
M = 1.6 L/D = 4.25	1	1500	146	.30	1133	.22	1209	.25
	2	2500	146	.49	2643	.52	2820	.57
	3	4100	158	.81	4154	.82	4431	.90
	4	5500	160	1.09	5664	1.12	6043	1.23
	5	6900	146	1.42	7174	1.42	7654	1.56
	6	8200	142	1.62	8685	1.72	9265	1.88
	7	9600	144	1.90	10195	2.01	10877	2.21
M = 1.9 L/D = 2	1	-----	---	---	2624	.21	2994	.23
	2	5350	173	.42	6122	.48	6987	.55
	3	9800	152	.77	9619	.75	10980	.86

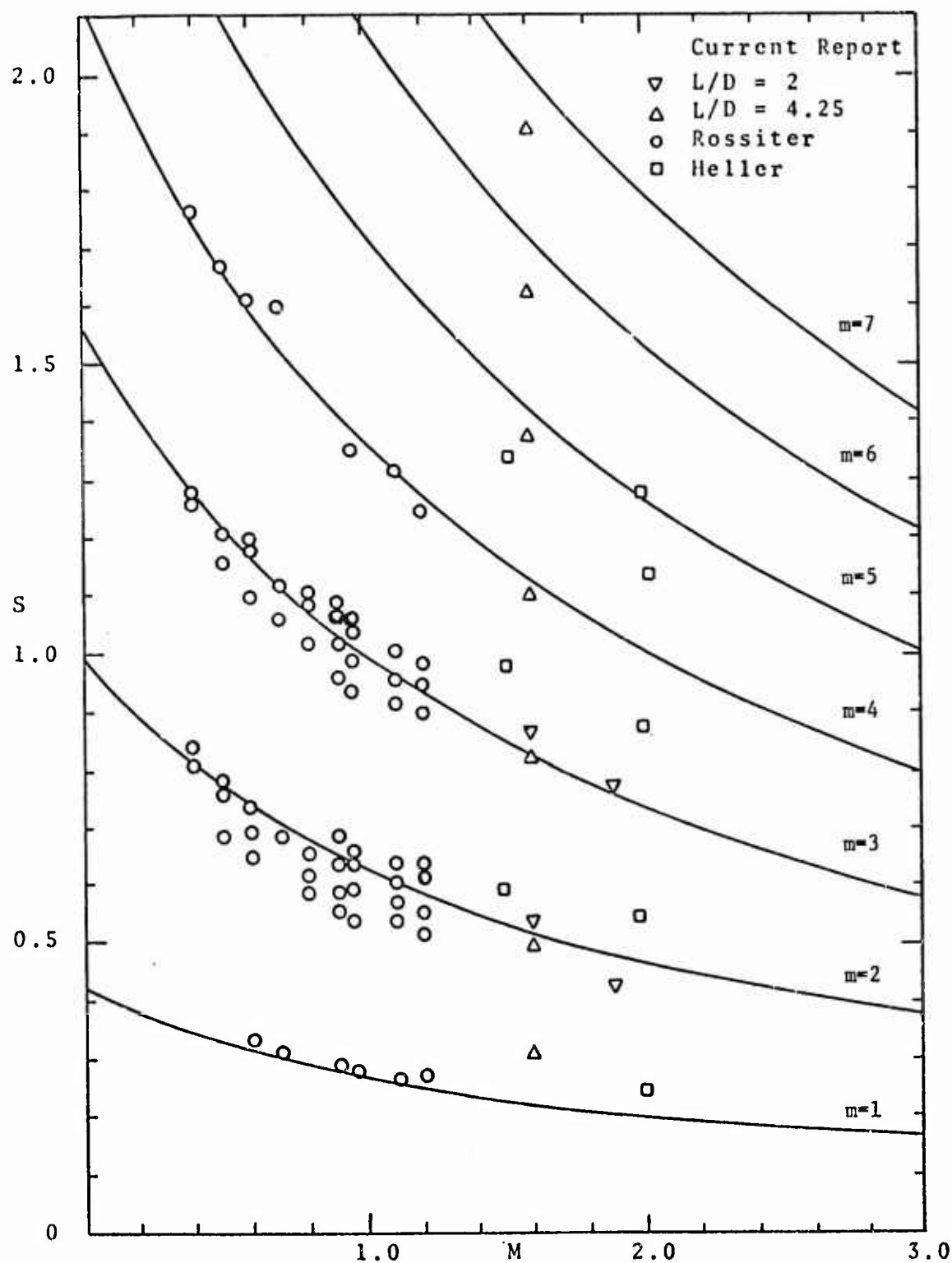


Fig. 16. Nondimensional Resonant Frequencies as a Function of Mach Number with Implementation of Rossiter's Formula.

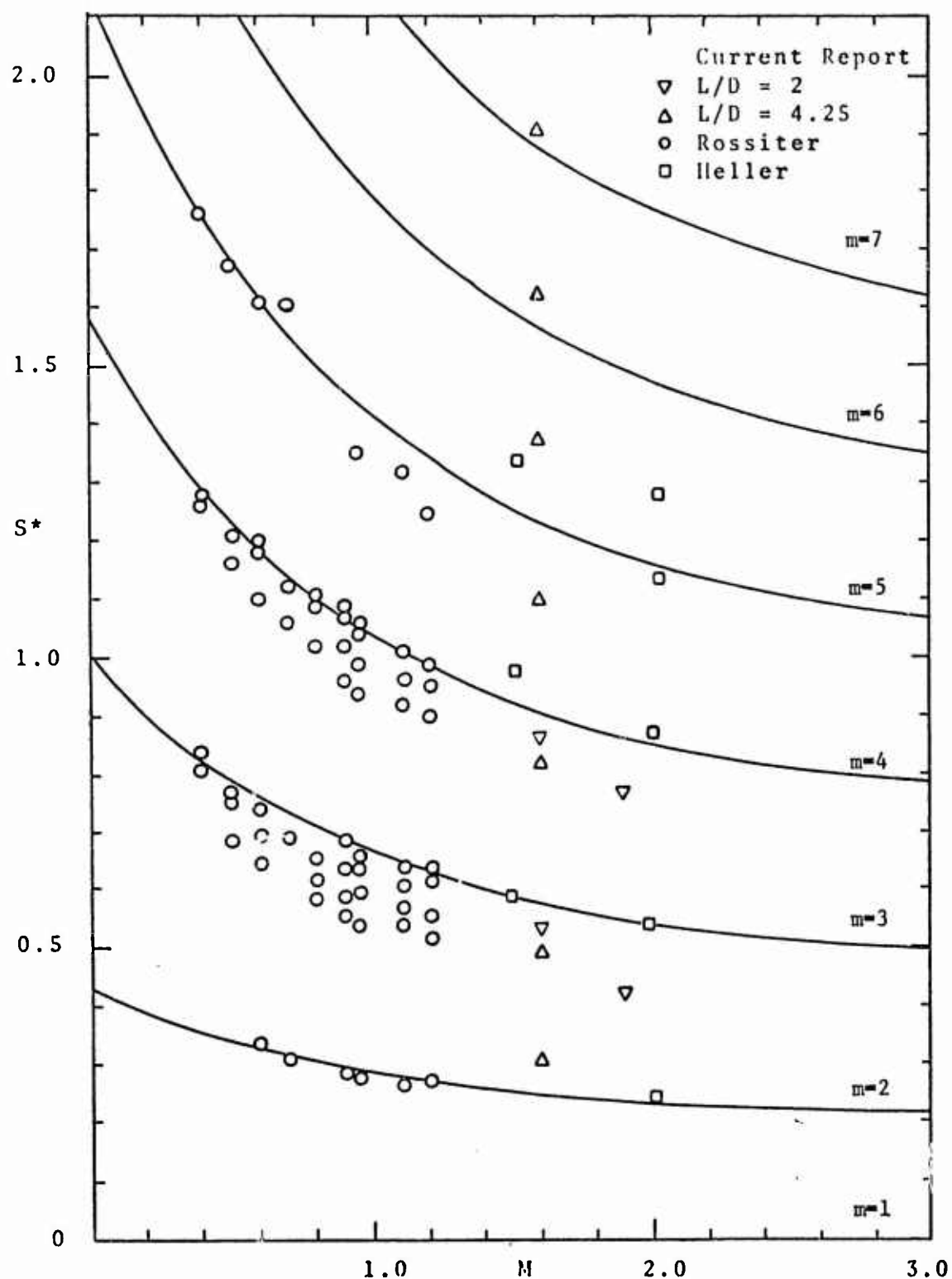


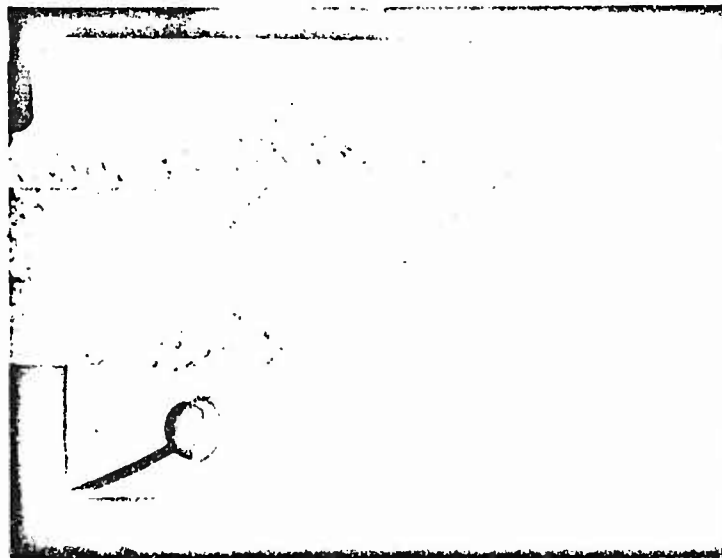
Fig. 17. Nondimensional Resonant Frequencies as a Function of Mach Number with Implementation of Modified Rossiter Formula.

The frequency and Strouhal number information obtained from these equations for the present test conditions are shown in Table I. From Table I and Figs. 16 and 17, the present data are seen to agree better with Rossiter's equation and data.

Oscillation Reduction Effectiveness. The effectiveness of the modified cavity configurations in reducing oscillations is seen by comparing schlieren photographs and amplitude vs. frequency plots with similar photographs and plots of a rectangular cavity.

Figure 18 shows a comparison of schlieren photographs of the flow over a rectangular cavity and a cavity with 15 degree ramps into the cavity at the leading and trailing edges (configuration 6, Fig. 12). Both cavities have an $L/D = 2$ and a freestream Mach number of 1.6. These photographs show that the shear layer over the rectangular cavity is wavy as described in the sketches of Fig. 14. The shear layer over the ramped cavity, however, is straight. A comparison of the frequency plots for these two cavities, Fig. 19, shows the background noise level is about the same for both cavities, but the discrete frequencies of 5600 and 9300 Hz which are present in the rectangular cavity have been eliminated in the ramped cavity. This represents a reduction of 23 dB at 5600 Hz and 6 dB at 9300 Hz.

Schlieren photographs for these same cavities for a flow Mach number of 1.9, Fig. 20, show that the shear layer



(a)



(b)

Fig. 18. Schlieren Photographs - Shear Layer above
(a) Rectangular Cavity; (b) Ramped
Cavity; $M = 1.6$; $L/D = 2$.

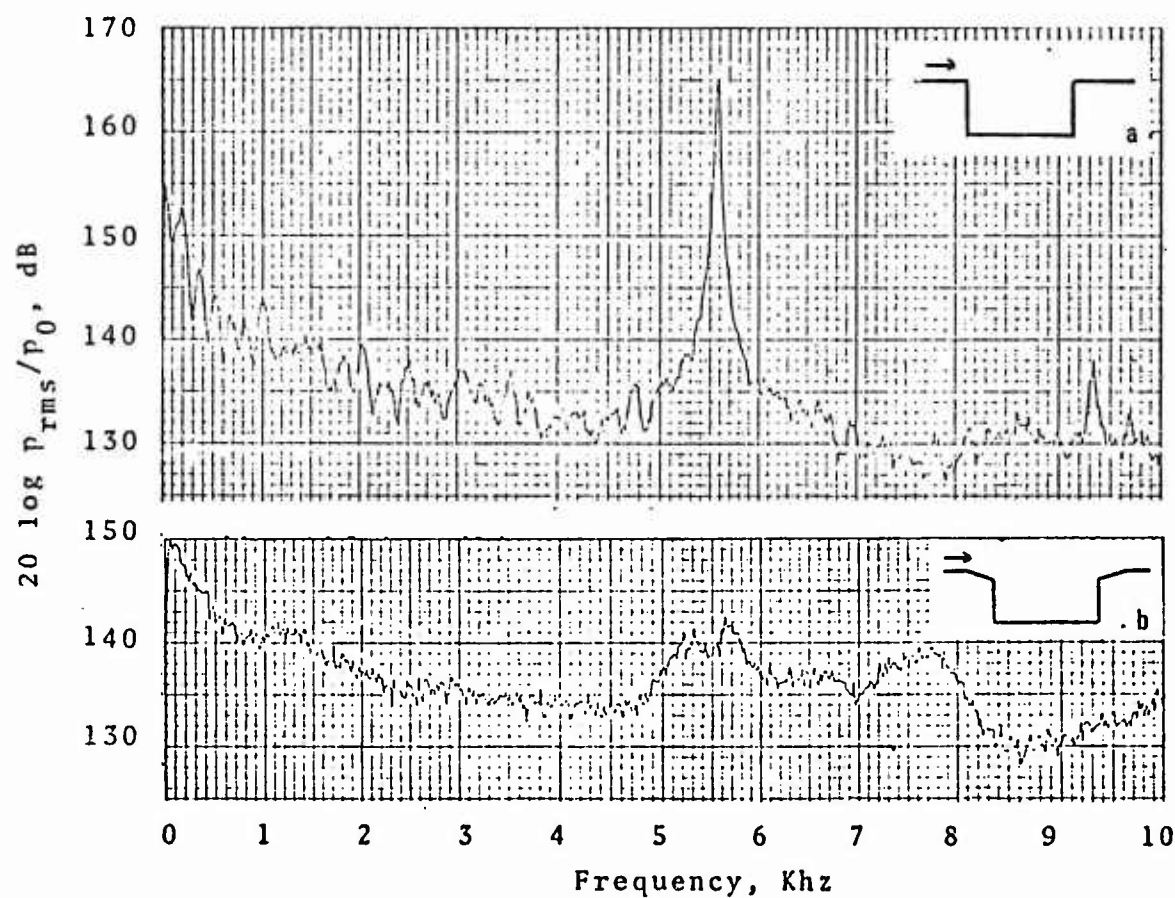


Fig. 19. Narrow Band Spectra - (a) Rectangular Cavity; (b) Ramped Cavity; $M = 1.6$; $L/D = 2$.

Reproduced from
best available copy.

(a)



(b)

Fig. 20. Schlieren Photographs - Shear Layer above
(a) Rectangular Cavity; (b) Ramped
Cavity; $M = 1.9$; $L/D = 2$.

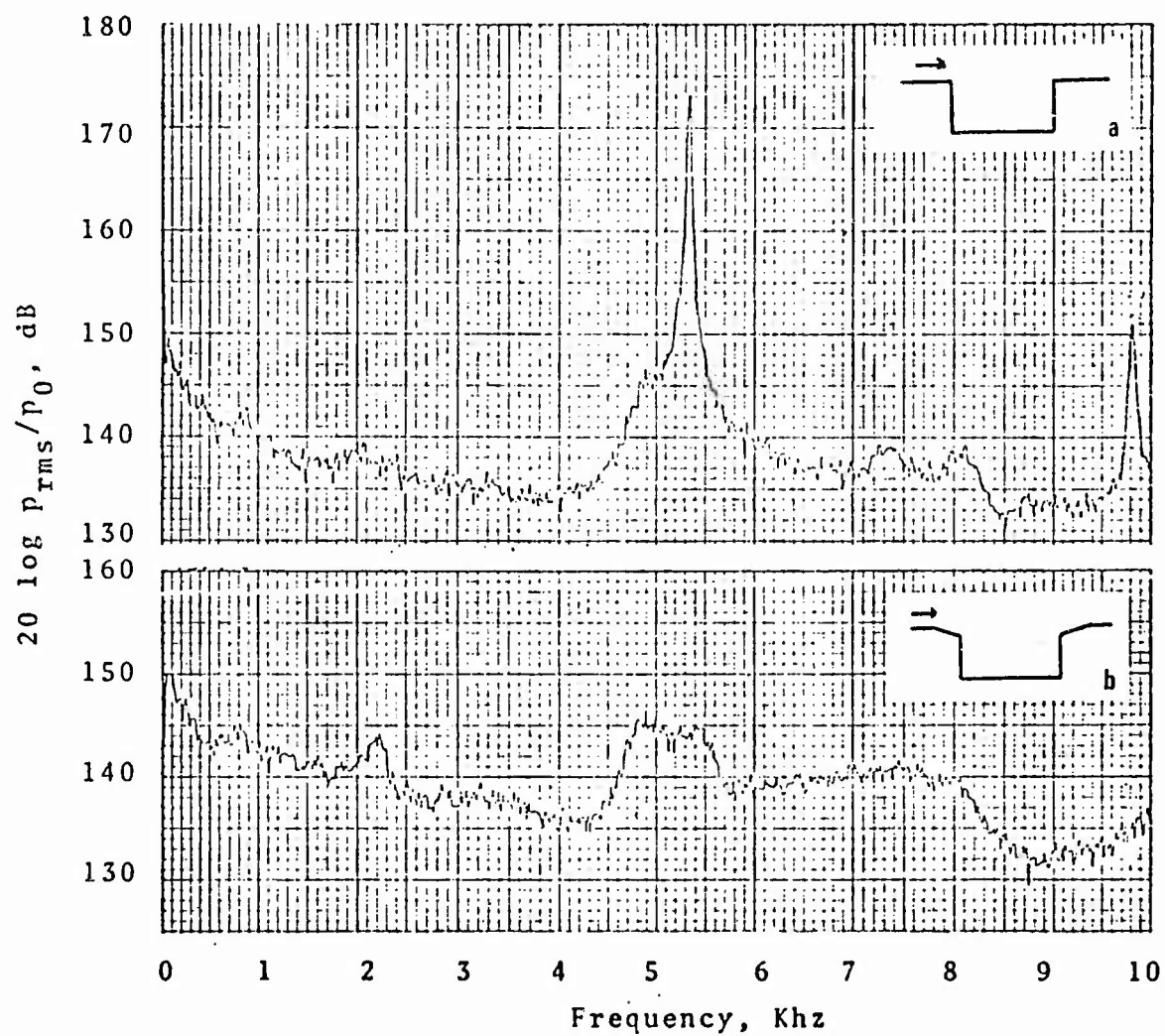


Fig. 21. Narrow Band Spectra - (a) Rectangular Cavity; (b) Ramped Cavity; $M = 1.9$; $L/D = 2$.

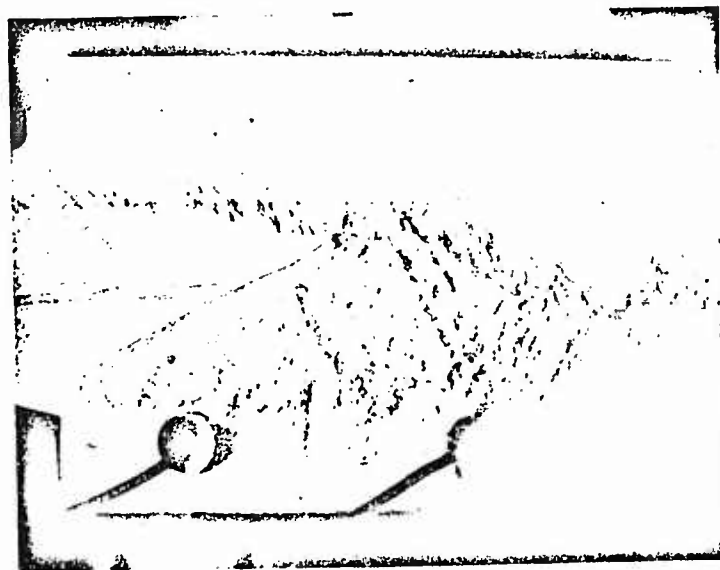
over the rectangular cavity is again wavy while the shear layer over the ramped cavity is straight. Figure 21 shows a comparison of the frequency plots for these cavities at $M = 1.9$. Again the discrete frequencies which are present in the rectangular cavity have been eliminated in the ramped cavity. This represents a reduction of 28 dB at 5300 Hz and 16 dB at 9800 Hz.

Figure 22 compares schlieren photographs for cavities with $L/D = 4.25$ and $M = 1.6$. Again the shear layer is wavy over the rectangular cavity and straight over the ramped cavity. A comparison of the frequency plots, Fig. 23, shows several frequency modes are present in the rectangular cavity but all of these are eliminated in the ramped cavity. This represents a reduction of 15 dB in the mode 3 and 4 frequencies and lesser amounts in the other modes.

Schlieren photographs of the configurations with a 15 degree ramp away from the cavity at the leading edge (configurations 4 and 5, Fig. 12) are shown in Fig. 24. Photographs a and c in this figure show the shear layer to be straight and photographs b and d show the shear layer to be wavy. Figure 25 shows frequency plots for these configurations. Plots a and c, which correspond to photographs a and c in Fig. 24, show no discrete frequencies in these cavities. Plots b and d, which correspond to photographs b and d with the wavy shear layer, show the presence of discrete frequencies in the cavities. These figures show that L/D is very



(a)



(b)

Fig. 22. Schlieren Photographs - Shear Layer above
(a) Rectangular Cavity; (b) Ramped Cavity;
 $M = 1.6$; $L/D = 4.25$.

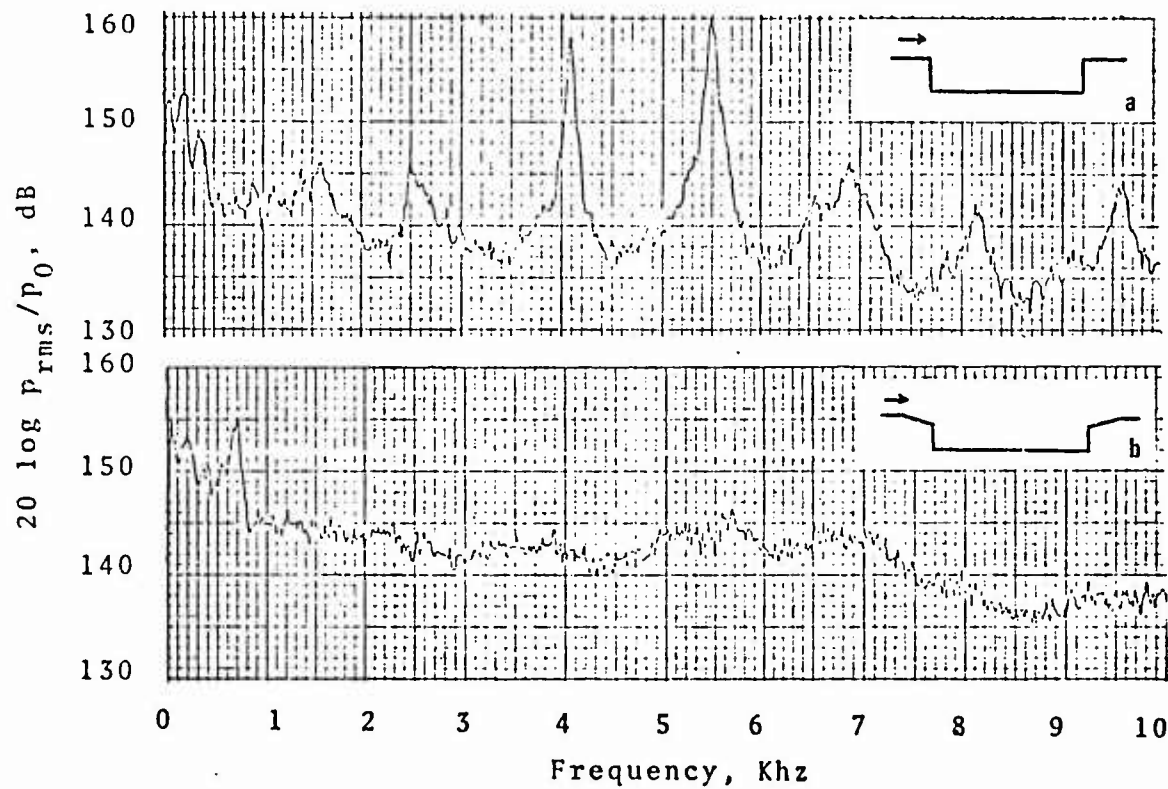


Fig. 23. Narrow Band Spectra - (a) Rectangular Cavity; (b) Ramped Cavity; $M = 1.6$; $L/D = 4.25$.

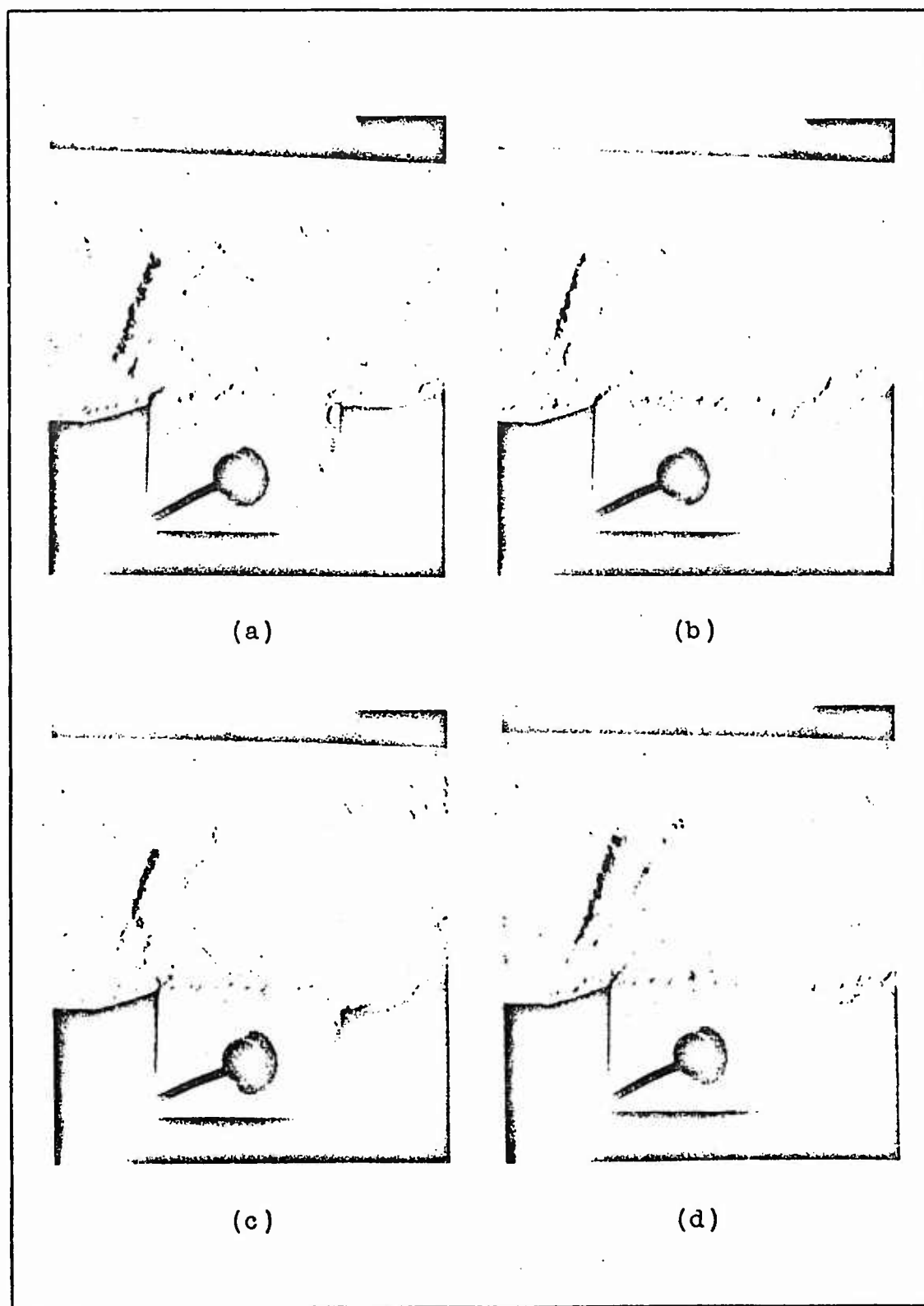


Fig. 24. Schlieren Photographs - Rectangular Cavity
with Leading Edge Ramp; $M = 1.6$;
(a) $L/D = 1.6$; (b) $L/D = 2.4$; (c) $L/D = 1.9$;
(d) $L/D = 2.8$.

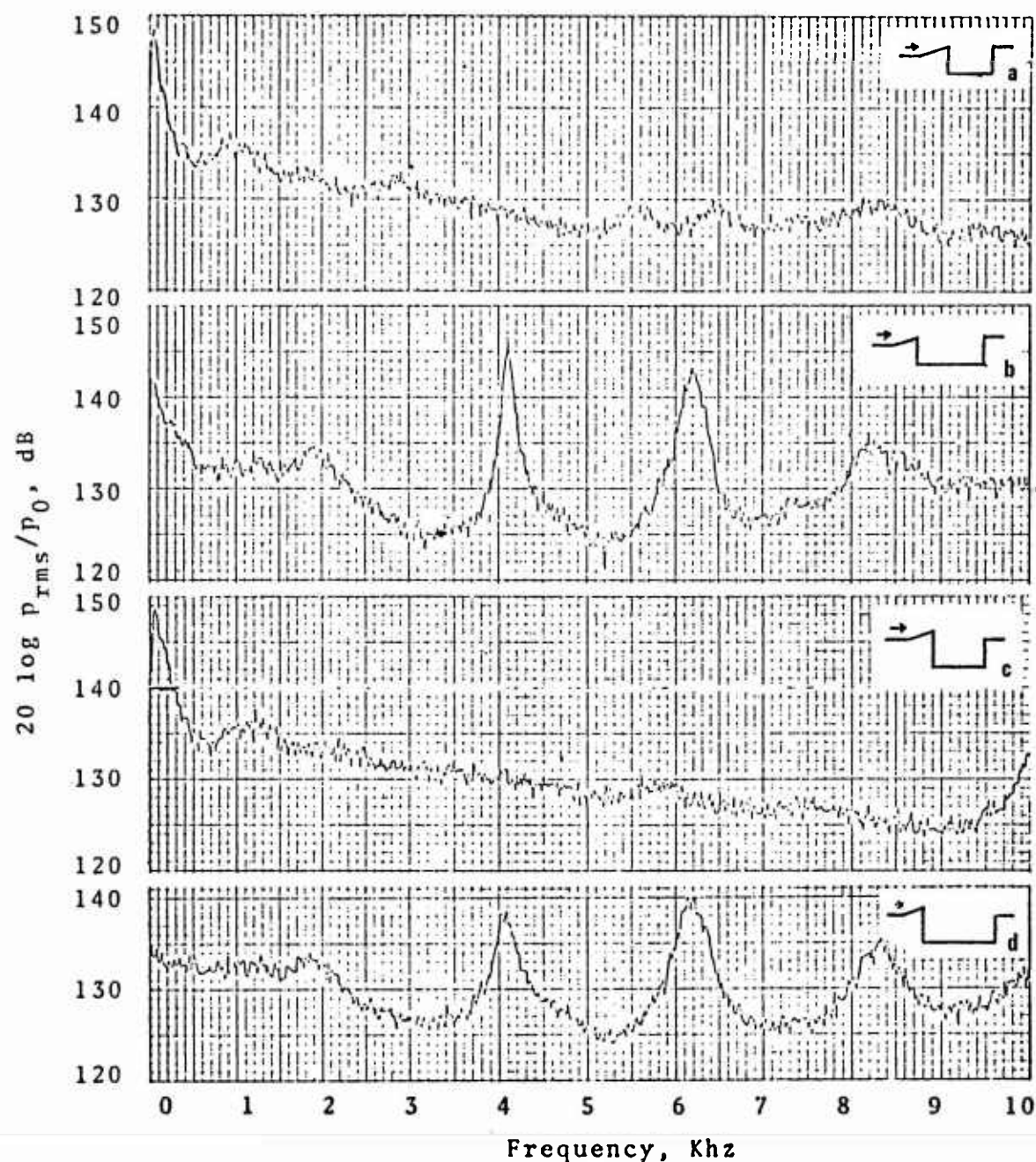


Fig. 25. Narrow Band Spectra - Rectangular Cavity with Leading Edge Ramp; $M = 1.6$; (a) $L/D = 1.6$; (b) $L/D = 2.4$; (c) $L/D = 1.9$; (d) $L/D = 2.8$.

critical to the effectiveness of this type ramp in reducing oscillations. An increase of only 50 percent in L/D induced discrete frequencies in these configurations. Even at the higher L/D , however, the maximum levels of the discrete frequencies were reduced 20 - 25 dB from the levels of the corresponding modes in the rectangular cavity.

Results for two closely spaced cavities, one immediately behind the other, are shown in Figs. 26 through 30. Figure 26 shows that both cavities have the same discrete frequencies and that these frequencies are the same as for a single cavity with the same L/D and Mach number. This confirms the results obtained on the water table.

Schlieren photographs of double rectangular and double ramped cavities are shown in Fig. 27 for a Mach number of 6 and in Fig. 28 for a Mach number of 1.9. The shear layers over the rectangular cavities at both Mach numbers again are wavy. The shear layers over the ramped cavities are also wavy which would indicate the presence of oscillations within the cavities. A comparison of the frequency plots in Fig. 29 for $M = 1.6$ and Fig. 30 for $M = 1.9$, shows that oscillations are present in the ramped cavities as well as in the rectangular cavities. Even so, at $M = 1.9$, the amplitude of the mode 2 frequency was reduced 24 dB in the front ramped cavity and 12 dB in the rear ramped cavity while the mode 3 frequency was reduced 18 dB in the front ramped cavity. At $M = 1.6$, however, the reduction in the

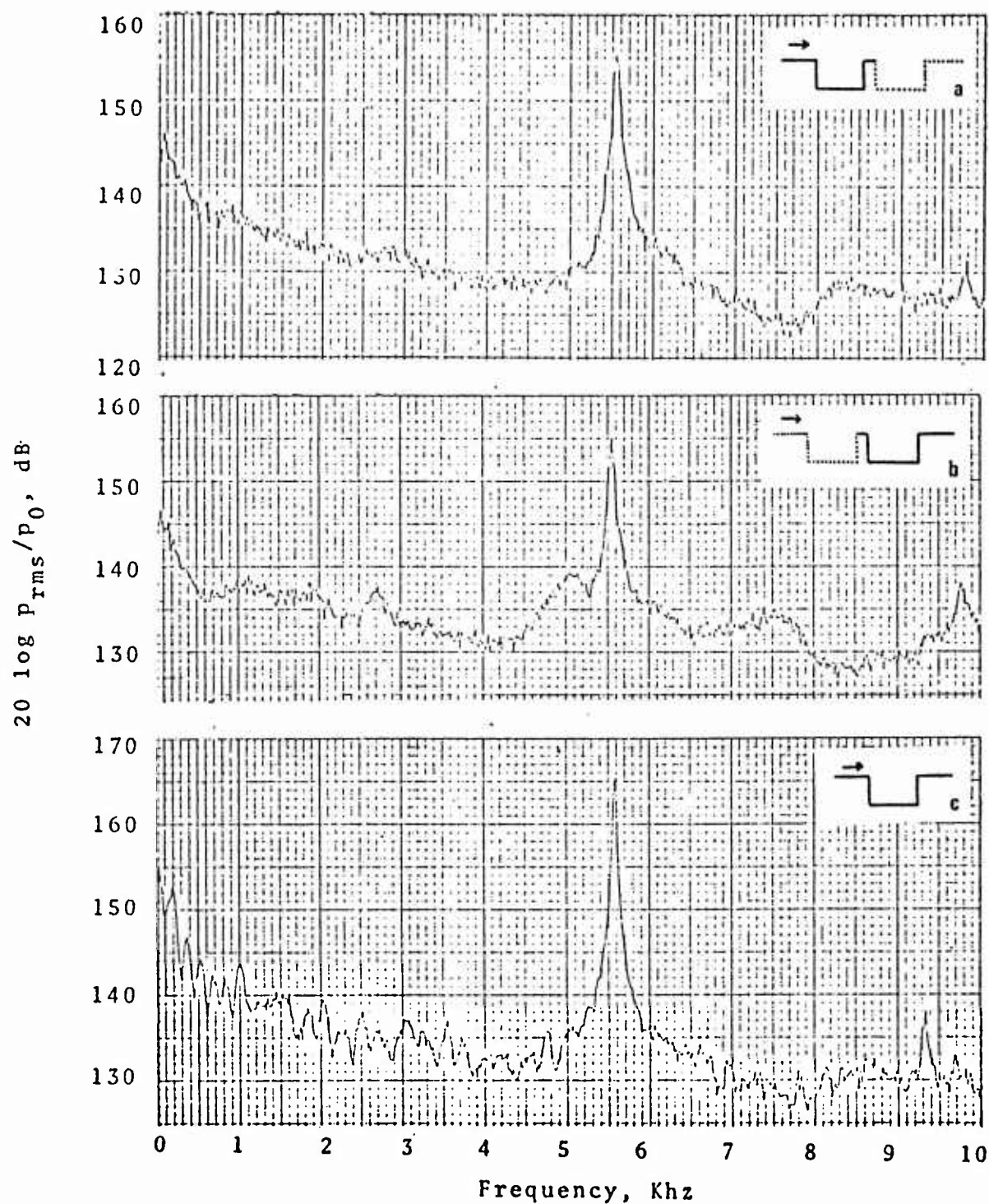
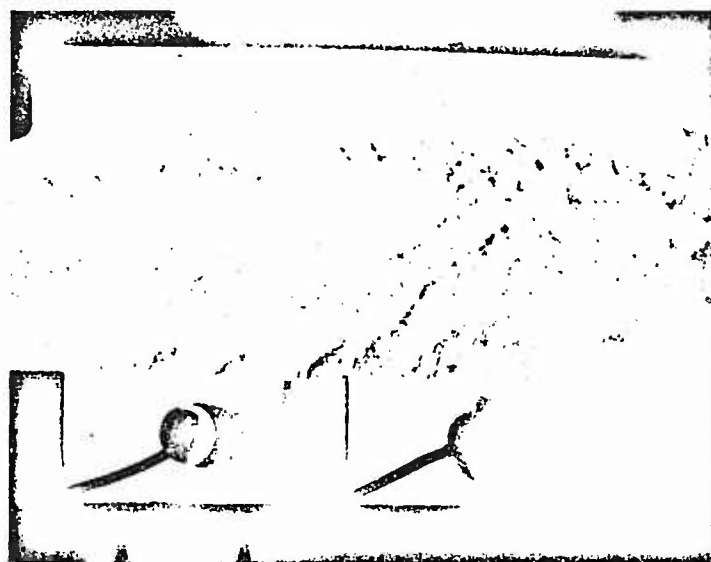


Fig. 26. Narrow Band Spectra - Double Rectangular Cavities - (a) Forward Cavity; (b) Rear Cavity; Single Rectangular Cavity; $M = 1.6$; $L/D = 2$.



(a)



(b)

Fig. 27. Schlieren Photographs - Double
Cavities - (a) Rectangular; (b) Ramped;
 $M = 1.6$; $L/D = 2$.

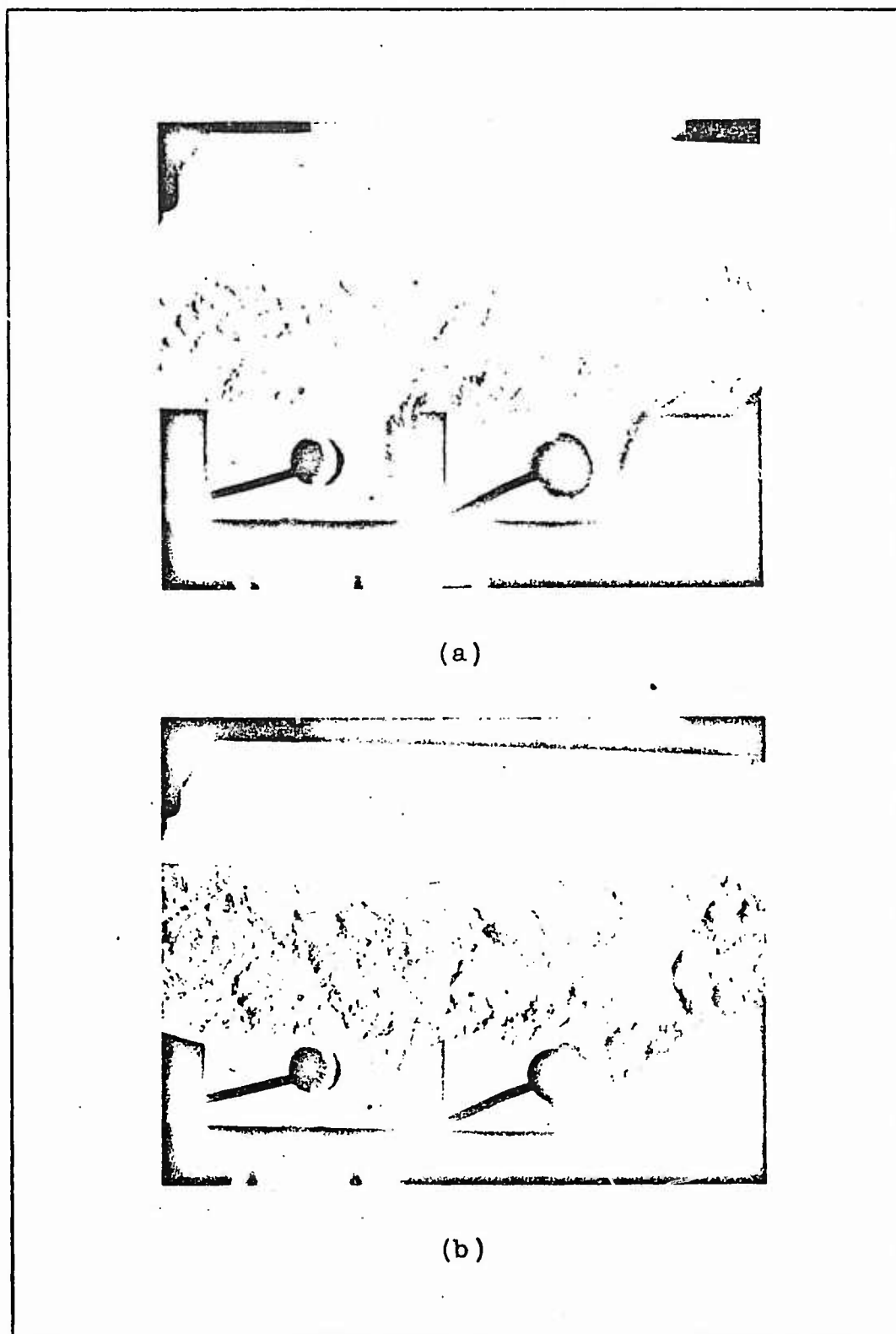


Fig. 28. Schlieren Photographs - Double Cavities - (a) Rectangular; (b) Ramped; $M = 1.9$; $L/D = 2$.

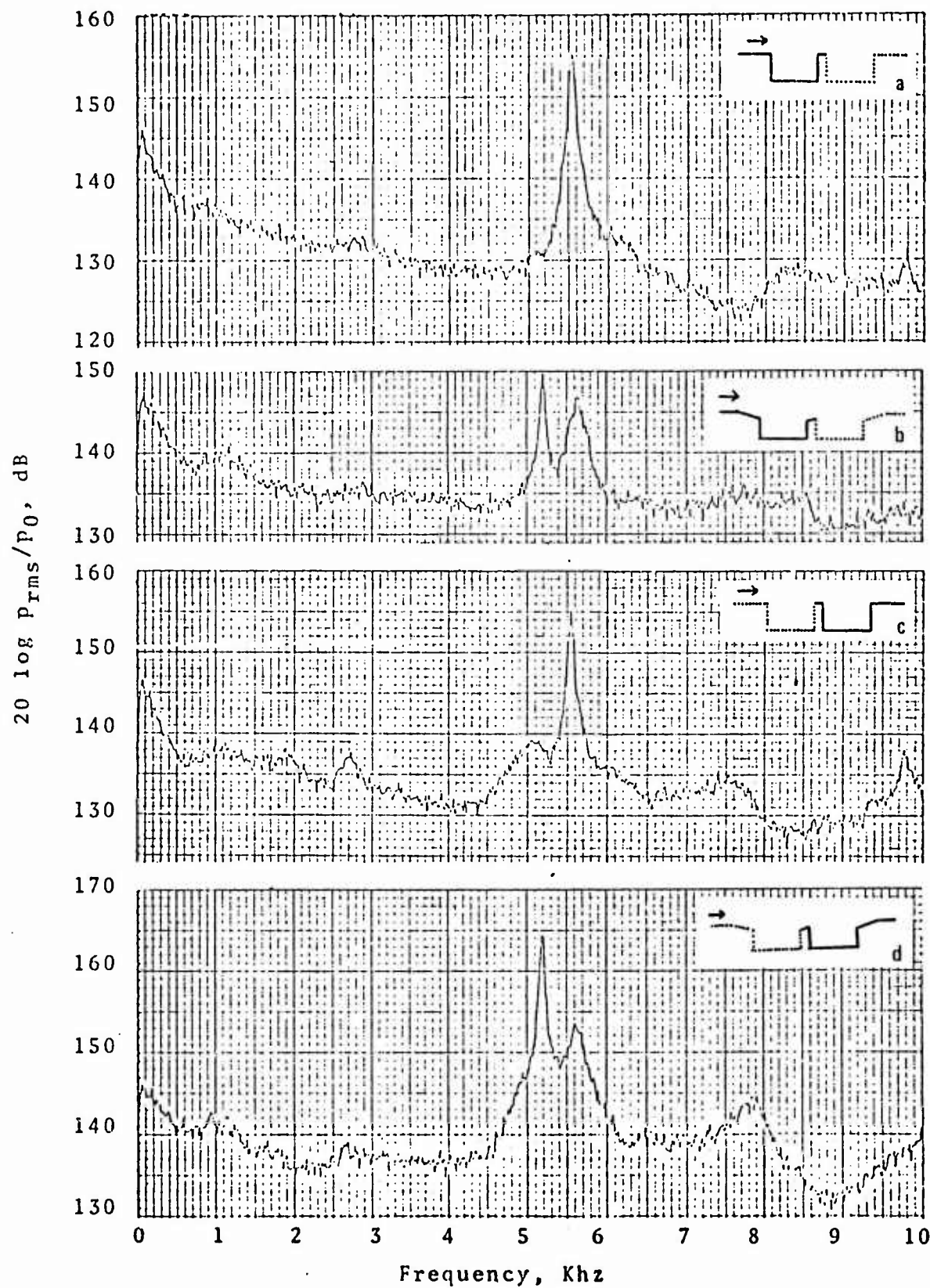


Fig. 29. Narrow Band Spectra - Double Cavities - (a) Forward Rectangular Cavity; (b) Forward Ramped Cavity; (c) Rear Rectangular Cavity; (d) Rear Ramped Cavity; $M = 1.6$; $L/D = 2$.

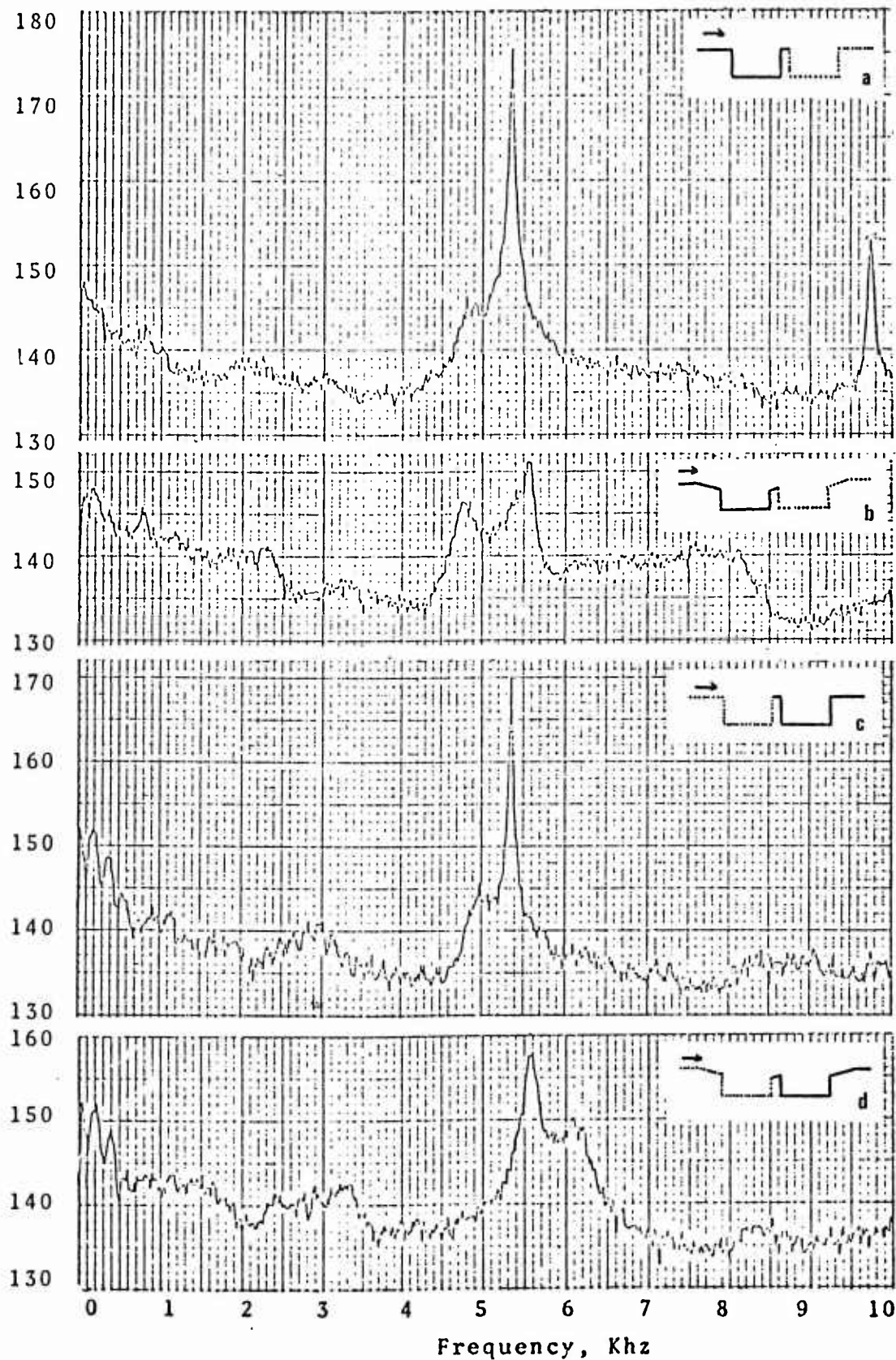


Fig. 30. Narrow Band Spectra - Double Cavities - (a) Forward Rectangular Cavity; (b) Forward Ramped Cavity; (c) Rear Rectangular Cavity; (d) Rear Ramped Cavity; $M = 1.9$; $L/D = 2$.


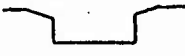


mode 2 frequency of the front cavity was only 5 dB and the rear cavity showed an increase of 9 dB.

Table II gives the peak amplitude for the frequency modes present in the various single cavity configurations tested. From this table the effectiveness of each configuration in reducing the amplitude of the discrete frequencies within the cavity can be seen. Table III gives similar information for double cavity configurations.



Table II

Mode Frequency Amplitudes for
Single Cavity Configurations

$M = 1.6; L/D = 2$

	Mode No. 2	3
	165 dB	138 dB
	142 dB	132 dB
	129 dB	127 dB
	131 dB	126 dB

$M = 1.9; L/D = 2$

	Mode No. 2	3
	173 dB	152 dB
	145 dB	136 dB

$M = 1.6; L/D = 4.25$




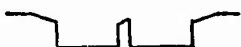
Mode No.		
1	146 dB	145 dB
2	146 dB	144 dB
3	158 dB	143 dB
4	160 dB	145 dB
5	146 dB	144 dB
6	142 dB	139 dB
7	144 dB	138 dB



Table III

Mode Frequency Amplitudes for
Double Cavity Configurations

M = 1.6; L/D = 2

	Front		Rear	
Mode No.	2	3	2	3
	155 dB	132 dB	155 dB	138 dB
	150 dB	134 dB	164 dB	138 dB

M = 1.9; L/D = 2

	Front		Rear	
Mode No.	2	3	2	3
	176 dB	153 dB	170 dB	---
	151 dB	135 dB	158 dB	---

VI. Conclusions

Motion pictures of the flow over cavities on the water table show that the water table can be used to predict the response of cavities to air flow over them. In particular, it is possible to monitor and analyze the oscillatory motion of the shear layer, to observe the mass-injection and mass-ejection process near the trailing edge, and to observe the generation and upstream propagation of a pressure wave within the cavity and its reflection from the leading edge.

The sequence of events for cavity oscillations based on the water table tests clearly associates the cavity pressure oscillations with the transverse oscillations of the shear layer.

Two cavities, one immediately behind the other, oscillate in phase. Apparently the disturbances introduced into the flow by the upstream shear layer tend to control the phase of oscillations in the downstream cavity.

The cavity configurations which caused the worst oscillations were those that drew the shear layer deeper into the cavity. Configurations which caused the shear layer to reattach after the trailing edge, however, showed no oscillations within the cavity. An airfoil at a negative angle of attack or a ramp away from the mouth of the cavity located in front of the leading edge were effective in keeping the shear layer out of the cavity, but these configurations depended critically on Mach number and cavity length.

Reducing or eliminating the transverse oscillations of the shear layer over the cavity is another means to reduce cavity oscillations. This can be accomplished in several ways. Positioning a half-cylindrical cowl, an airfoil, or a baffle in front of the trailing edge proved effective in stabilizing the shear layer. The location of these, however, was dependent on Mach number. The most effective configuration found for stabilizing the shear layer was a cavity with 15 degree beveled leading and trailing edges.

VII. Recommendations

Based on the results of this investigation it is recommended that preliminary testing of cavity designs be accomplished on the water table. Besides providing good qualitative information on the flow over cavities, water table tests can be conducted in much less time and at a fraction of the cost of wind tunnel tests.

An investigation should be conducted to determine the reason that a cavity with leading and trailing edge ramps is effective in stabilizing the shear layer. The possibility that vortices are not shed at the leading edge should be investigated.

Further air flow studies should be conducted on those configurations which reduced oscillations on the water table but were not tested in air. Also, many other possible means to stabilize the shear layer exist. A systematic study should be conducted of other likely design configurations comparing not only effectiveness in reducing oscillations but also the feasibility of applying the designs to aircraft without causing other problems such as increased drag.

Bibliography

1. Karamcheti, K. "Acoustic Radiation from Two-Dimensional Rectangular Cutouts in Aerodynamic Surfaces", NACA TN 3487, August 1955.
2. Heller, H. H., G. Holmes, and E. E. Covert. "Flow-Induced Pressure Oscillations in Shallow Cavities", Flight Dynamics Laboratory, Vehicle Dynamics Division, Air Force Systems Command, Wright-Patterson AFB, Ohio, AFFDL-TR-70-104, December 1970.
3. Covert, E. E. "An Approximate Calculation of the Onset Velocity of Cavity Oscillations", AIAA Journal, 8:2189-2194 (December 1970).
4. Roshko, A. "Some Measurements of Flow in a Rectangular Cutout", NACA TN 3488, August 1955.
5. Charwat, A. F., et al. "An Investigation of Separated Flows - Part I: The Pressure Field", Journal of Aerospace Sciences, 28:457-470 (June 1961).
6. Maull, D. J. and L. F. East. "Three Dimensional Flow in Cavities", Journal of Fluid Mechanics, 16:620-632 (August 1963).
7. Bruce, P. W. Flow Visualization in Axial-Flow Compressor and Turbine Cascades Utilizing the Water Table. Unpublished Thesis. Wright-Patterson Air Force Base, Ohio: Air Force Institute of Technology, December 1973.
8. Warren, C. H. "Application of the Hydraulic Analogy to Internal Subsonic Flow", Army Inertial Guidance and Control Laboratory, Research and Development Directorate, U. S. Army Missile Command, Redstone Arsenal, Alabama, RG-TR-67-19, July 1967.
9. Quinn, B. "Flow in the Orifice of a Resonant Cavity", AIAA Student Journal, 1:1-5 (January 1963).
10. East, L. F. "Aerodynamically Induced Resonance in Rectangular Cavities", Journal of Sound and Vibration, 3: 277-287 (March 1966).

Vita

Dennis Lynn Carr was born [REDACTED] [REDACTED]

[REDACTED] He was graduated from Syracuse University in 1967 with a Bachelor of Science degree in Aerospace Engineering. He completed pilot training in 1968 and served as a T-38 instructor pilot until 1971. He spent 1972 in Southeast Asia as a B-57 aircraft commander. He entered the Air Force Institute of Technology in March 1973.

Permanent address: [REDACTED]
[REDACTED] [REDACTED] [REDACTED]

This thesis was typed by Jane Manemann.